Selection of Ethanol Tolerant Strains of *Candida albicans* by Repeated Ethanol Exposure Results in Strains with Reduced Susceptibility to Fluconazole

Andrew W. Day[1,2] and Carol A. Kumamoto[2*]

[1]Graduate School of Biomedical Sciences, Tufts University, Boston, Massachusetts, 02111, USA

[2]Department of Molecular Biology and Microbiology, Tufts University, Boston, Massachusetts, 02111, USA

*Correspondence to Carol A. Kumamoto, Department of Molecular Biology and Microbiology, Tufts University, 150 Harrison Ave., Boston, MA, 02111, USA, carol.kumamoto@tufts.edu

Short Title: *Candida albicans* Ethanol Response and Altered Fluconazole susceptibility

Keywords: *Candida albicans*, antifungal resistance, ethanol tolerance, evolution

Abstract

Candida albicans is a commensal yeast that has important impacts on host metabolism and immune function, and can establish life-threatening infections in immunocompromised individuals. Previously, *C. albicans* colonization has been shown to contribute to the progression and severity of alcoholic liver disease. However, relatively little is known about how *C. albicans* responds to changing environmental conditions in the GI tract of individuals with alcohol use disorder, namely repeated exposure to ethanol. In this study, we repeatedly exposed *C. albicans* to high concentrations (10% vol/vol) of ethanol—a concentration that can be observed in the upper GI tract of humans following consumption of alcohol. Following this repeated exposure protocol, ethanol small colony (Esc) variants of *C. albicans* isolated from these populations exhibited increased ethanol tolerance, altered transcriptional responses to ethanol, and cross-resistance/tolerance to the frontline antifungal fluconazole. These Esc strains exhibited chromosomal copy number variations and carried polymorphisms in genes previously associated with the acquisition of fluconazole resistance during human infection. This study identifies a selective pressure that can result in evolution of fluconazole tolerance and resistance without previous exposure to the drug.

Introduction

Candida albicans is an opportunistic pathogen causing severe morbidity and mortality in immunocompromised patients. *Candida spp* are the second most common cause of nosocomial bloodstream infection in the US, and cause about 70% of all fungal infections [1,2]. The most common species causing these fungal infections is *C. albicans*, the causative agent of oral thrush, vulvovaginitis, and bloodstream infections which result in mortality rates in immunocompromised patients ranging from roughly 30-56% [3–5]. Before *C. albicans* causes

52 deadly bloodstream infections, it establishes commensalism within the gastrointestinal tract of
53 humans [6,7]. Importantly, rates of antifungal resistance among *C. albicans* isolates have been
54 rising throughout recent years [8], contributing to difficulty in treating bloodstream infections.
55 Therefore, it is important to investigate factors that promote antifungal resistance whether
56 acquired during infection or the preceding commensal state.

57 *C. albicans* commensalism has been studied particularly in disease states which
58 predispose individuals to bloodstream infections. However, the environmental conditions in the
59 GI tract and how they contribute to fungal physiology have been less studied. One condition of
60 interest is the GI tract of individuals with alcohol use disorder (AUD). Recently, changes in the
61 gut microbiome of individuals with alcohol use disorder, including a loss of fungal diversity, and
62 blooms of *C. albicans* have been noted [9–11]. *C. albicans* blooms in the alcoholic GI tract
63 promote the progression and increase the severity of alcoholic liver disease. Anti-
64 *Saccharomyces cerevisiae* IgG antibodies (ASCA), which are thought to be broadly induced by
65 fungi, show an inverse correlation with 6-month and 5-year survival rates in patients with
66 alcoholic cirrhosis [9,10]. These findings suggest that fungal colonization can exacerbate
67 diseases associated with alcohol use and abuse. However, there are still many questions
68 surrounding why *C. albicans* relative abundance increases in the alcoholic GI tract and how *C.*
69 *albicans* responds to environmental changes in the alcoholic GI tract.

70 One of the most intuitive features of the environment in the alcoholic GI tract is the
71 increased presence of ethanol that members of the microbiota from the mouth through the
72 proximal small intestine would be exposed to during bouts of consumption. Following
73 consumption of one to two standard drinks of ethanol, the percentage of alcohol in the stomach
74 and the small intestine can reach concentrations of roughly 10% ethanol [12,13]. To test how *C.*
75 *albicans* responds to conditions that mimic this environment, we repeatedly cultured C. albicans
76 in media with increasing amounts of ethanol, up to 10%. Model organisms such as *Escherichia*
77 *coli* and *Saccharomyces cerevisiae* have been shown to evolve increased ethanol tolerance as

78 a result of repeated exposure to ethanol [14,15]. We therefore hypothesized that *C. albicans*
79 would evolve increased ethanol tolerance following repeated exposure to ethanol.
80 In this study, we find that populations of *C. albicans* cells repeatedly exposed to ethanol
81 evolve increased ethanol tolerance. One ethanol tolerant strain showed increased ergosterol
82 content during exposure to ethanol. We show that increased ergosterol content, whether
83 induced by chemical stimulation or gain-of-function mutation, resulted in increased ethanol
84 survival of *C. albicans*. Whole genome sequencing of strains with increased ethanol tolerance
85 showed that these strains carried various chromosomal aneuploidies, some of which have been
86 observed in fluconazole resistant and tolerant strains of *C. albicans*, and single nucleotide
87 polymorphisms (SNPs). We also showed that the ethanol tolerant strains exhibited increased
88 resistance and tolerance to azole drugs but not caspofungin or amphotericin B. These results
89 suggest that *C. albicans* exposed to ethanol in the alcoholic GI tract could exhibit fluconazole
90 resistance without previously being exposed to the antifungal drug.
91

92 # Results

93 **Selection of ethanol tolerant *C. albicans* isolates**

94 The ability of *C. albicans* to evolve an altered response to ethanol exposure was
95 investigated. To this end, *C. albicans* strain SC5314 was cultured eight times for 4 hrs each in
96 tissue culture medium with 10% fetal bovine serum and 1X non-essential amino acids (referred
97 to as medium A) with or without increasing concentrations of ethanol, as described in Materials
98 and Methods (**Fig. 1A).** This process was repeated with five independent populations of cells.

99 **Figure 1 Isolation of Ethanol Tolerant Strains. A)** The repeated ethanol exposure
100 protocol is illustrated. 10^6 cells of *C. albicans* strain SC5314 from 5 different biological replicate
101 populations were inoculated into medium A with increasing concentrations of ethanol (1-10%
102 vol/vol) or medium A diluted with water. Populations were exposed to 8 passages in ethanol or

103 paired mock-exposed populations exposed to 8 passages in media with water. After each 4
104 hour ethanol or water exposure step, cells were seeded into YPD for recovery, and cultures
105 were plated onto YPD-agar for examination of the populations. Recovery cultures were grown to
106 post-exponential phase, and a glycerol stock was made. Cells from the recovery culture were
107 then used for the next step. **B)** Relative survival of ethanol small colony (Esc) strains following a
108 4-hour ethanol exposure relative to WT ethanol survival was measured as described in
109 Materials and Methods. Symbols show results from biological replicate cultures, bars show
110 mean with standard deviation. Outliers were removed through ROUT, Q=1%, and statistical
111 significance calculated by Brown-Forsythe and Welch ANOVA test. Each group represents 16-
112 18 biological replicate cultures. (*, $p < 0.0170$; **, $p < 0.0037$; ***, $p < 0.0004$) **C)** Fraction of
113 survivors was measured for 8-16 biological replicate cultures for each point. Timepoints taken
114 were 0, 2, 4, 6, 8, 10, 12, or 24 hours of incubation time in 10% ethanol. Error bars show
115 standard error for each timepoint. Horizontal line represents 90% death. Minimum duration of
116 killing 90% (MDK90) values are plotted as vertical lines with solid black line representing WT
117 and dashed lines representing Esc strains.

118 Throughout the repeated-ethanol exposure protocol, populations from each passage
119 were plated onto YPD agar to monitor population dynamics. An increased number of small-
120 sized colonies (50% of the size of normal sized colonies or less) was observed with greater
121 numbers of passages and higher concentrations of ethanol (**Supplemental Fig. S1**). Small-
122 sized colonies were rare in populations not exposed to ethanol. From these populations, small
123 and normal sized colonies were isolated to determine their properties.

124 Normal-sized colonies were isolated from four different populations exposed repeatedly
125 to ethanol, as well as from populations that were repeatedly exposed to water. Strains from
126 normal-sized colonies were grown to post-exponential phase and added to medium A containing
127 10% ethanol or 10% water as described in Materials and Methods. Following the four-hour ethanol

128 exposure at 37ºC in a 5% CO_2 atmosphere, cells were serially diluted, and plated to determine
129 CFU and percentage survival. The final CFU of the 10% water and 10% ethanol cultures were
130 counted and used to determine the final percentage survival of the ethanol cultures. Values were
131 standardized within each experiment to the survival of SC5314 in 10% ethanol (**Supplemental**
132 **Fig. S2**). Strains from normal-sized colonies from ethanol cultures showed no statistically
133 significant increase in ethanol survival compared to SC5314 survival and were not studied further.
134 Ethanol small colony (Esc) variants were purified from different populations and tested as
135 above to measure their ability to survive in ethanol. Relative survival values of SC5314, Esc6,
136 Esc7, and Esc8 are shown in **Fig. 1B**. Esc6, Esc7, and Esc8 were isolated from different,
137 independent populations and all showed significantly higher survival following the 4-hour ethanol
138 exposure, compared to the parent strain. The growth rates of these strains were measured in
139 YPD at 30ºC; the strains showed increases in doubling times ranging from 1.37 to 2.12X greater
140 than the doubling time of SC5314 shown in **Supplemental Fig. S3**.
141 The next experiment asked whether Esc strains had an increased ability to survive longer
142 exposures to ethanol. SC5314, Esc6, Esc7, and Esc8 were grown overnight and then subcultured
143 in medium A with 10% ethanol. CFU were determined for cultures at 0, 2, 4, 6, 8, 10, 12, and 24
144 hours of incubation. Fractions relative to the starting CFU of the cultures are shown in **Fig. 1C**.
145 The results showed that Esc6, Esc7, and Esc8 outperformed WT *C. albicans* in ethanol survival
146 from 0-6 hours and Esc7 and 8 were able to maintain higher ethanol survival relative to SC5314
147 through 24 hours. Esc6 had an early advantage in the first 6 hours compared to SC5314 but
148 began to die rapidly after 12 hours. A common way to measure tolerance to antibiotics in bacterial
149 systems is to determine the minimum duration of killing x fraction of the population (MDKx) [16].
150 We estimated the MDK90 for the strains by extrapolation and found that WT *C. albicans* had an
151 MDK90 of 10 hrs, Esc6 had an MDK90 of 12 hrs, Esc7 had an MDK90 of 16 hrs, and Esc8 had
152 an MDK90 of 19 hrs. These results showed that Esc7 and Esc8 had greater ethanol tolerance
153 than SC5314 and that Esc6 had slightly higher tolerance over the first 12 hours of exposure.

154 **Screen of Deletion Strains Reveals Pathways Important for Ethanol Survival**

155 Very little is known about factors that contribute to ethanol survival in *C. albicans* and
156 therefore, a screen of transcription factor deletion mutants [17] was conducted. Strains were
157 tested using the four-hour 10% ethanol exposure followed by plating on YPD-agar as described
158 above. Strains were selected for analysis if the deleted transcription factor was homologous to an
159 *S. cerevisiae* transcription factor with a role in ethanol survival, or if it regulated genes in pathways
160 with a known or hypothesized role in ethanol survival.

161 Ethanol survival experiments were performed for 18 different homozygous transcription
162 factor deletion strains and the wildtype strain, SN152 using six to twelve biological replicate
163 cultures for each strain. Results are shown in **Fig. 2.** Some of the transcriptional regulators that
164 are thought to be central to the *S. cerevisiae* ethanol response[18], e.g. *MSN4*, *MNL1 (scMSN2*
165 *analog*), and *CAP1* (*scYAP1 analog*) [18,19], were not necessary for ethanol survival in *C.*
166 *albicans*. Other deletion strains had an altered ability to survive in 10% ethanol. One strain,
167 deleted for *NDT80*, had a reduced ability to survive in ethanol, and four deletion strains (mutants
168 lacking *TYE7, ACE2, YOX1,* or *CRZ1)* had an increased ability to survive in ethanol. *ACE2* and
169 *CRZ1* knockout strains had particularly striking phenotypes with roughly 23 and 58-fold increases
170 in ethanol survival respectively compared to WT (SN152).

171 **Figure 2: Screen of the Ethanol Survival of Transcription Factor Deletion Strains.**
172 Strains described in Homann, et al [17] were exposed to 10% ethanol for four hours as previously
173 described. Relative survival was compared to SN152 (WT) as previously described. Relative
174 survival was log-transformed and graphed. Eighteen homozygous deletion mutants are graphed
175 with the name on the x-axis representing the deleted gene. Each point shows an individual
176 biological replicate culture, bars show mean values, and error bars show standard deviation. A
177 Brown-Forsythe and Welch ANOVA test was performed on log-transformed data to determine
178 statistical significance; * = $p < 0.0393$; ** = $p < 0.0016$; *** = $p < 0.0005$; **** = $p < 0.0001$.

179 To identify critical pathways for ethanol survival, we used previous studies to ask whether

180 pathways important for *S. cerevisiae* ethanol tolerance were regulated by these transcription
181 factors. It was found that all 5 transcription factors have been implicated in regulation of the
182 ergosterol pathway, either by co-expression studies, *ERG* promoter binding, or by computational
183 prediction [19–23]. Additionally, four out of the five transcription factors have putative roles in
184 biofilm formation, three in filamentous growth, two in cell-cell adhesion, two are involved with cell
185 wall synthesis/organization, and two with susceptibility to azoles based on results described in
186 the Candida Genome Database.

187 ***C. albicans* strains with elevated ergosterol levels exhibit increased ethanol tolerance**

188 In *S. cerevisiae,* increased ergosterol content confers greater ethanol tolerance and in
189 synthetic bilayers, increased ergosterol leads to lower membrane disruption [18,24–26]. Based
190 on our findings from the transcription factor deletion mutant screen, we hypothesized that
191 ergosterol is involved in *C. albicans* ethanol tolerance as well, and that Esc strains had alterations
192 in ergosterol levels. We therefore analyzed the ergosterol content in the ethanol tolerant strains.
193 SC5314 cells or Esc6, 7, 8 cells were cultured in medium A with 10% water or 10% ethanol for
194 four hours and ergosterol was extracted and quantitated as previously described [27,28].
195 Ergosterol quantity was calculated relative to SC5314 in 10% H2O and is shown in **Fig. 3A** (8
196 biological replicates from four different experiments). From these data, a statistically significant
197 increase in ergosterol content was seen in Esc7 in EtOH (p-value <0.0001, 2way ANOVA with
198 Dunnett's correction, mean = 1.77). Esc6 and Esc8 ergosterol content were not significantly
199 different from SC5314. These data support the model that higher levels of ergosterol in Esc7
200 promoted higher ethanol tolerance.

201 **Figure 3: Cells with increased ergosterol content show increased ethanol**
202 **tolerance. A)** Cells were grown for 4 hours in medium A with 10% ethanol or water and
203 harvested. Ergosterol was measured as a percentage ergosterol by mass normalized to wet-
204 pellet weight calculated as previously described [27,29,30] and Materials and Methods).
205 Relative ergosterol content was calculated by standardizing ergosterol % within each

206 experiment to SC5314 in 10% H2O. 4 separate experiments with 10 total biological replicate
207 cultures for each condition are shown. Symbols show individual replicate values relative to
208 SC5314 within the condition and bars show means with standard deviation (****, $p < 0.0001$).
209 Statistical significance calculated with 2way ANOVA with Dunnett's multiple comparison, only
210 significant comparisons are shown. **B)** Ethanol survival was measured after a 4-hr exposure of
211 SC5314 or SC5314 with a *UPC2* gain of function mutation (G648D) [31]. Relative survival was
212 standardized to SC5314 survival within each experiment. 11-12 biological replicates total from 3
213 different experiments are shown. One high outlier was removed from UPC2-G648D by ROUT
214 (Q=1%). Symbols show individual replicate cultures and bars show mean with standard
215 deviation (****, $p < 0.0001$). Statistical significance calculated by unpaired t-test. **C)** Ethanol
216 survival from SC5314 cells pre-treated for 4 hrs with DMSO or DMSO with 100ug/mL of
217 Artemisinin was measured. Each condition has 12 biological replicates. Ethanol exposure and
218 standardization are the same as in B. Symbols show standardized ethanol survival of individual
219 replicates and bars show median survival with error bars representing 95% confidence intervals.
220 Statistical significance was tested using a Mann-Whitney test (**, $p<0.0053$).

221 We therefore tested whether elevating ergosterol content in *C. albicans* through other
222 means would confer greater ethanol tolerance. One approach utilized an SC5314 strain with a
223 homozygous *UPC2* gain of function mutation (G648D; kind gift of J. Morschhauser). $UPC2_{G648D}$
224 results in increased ergosterol synthesis, and increased ergosterol content through upregulation
225 of *ERG11* [31]. Four hour ethanol survival of the SC5314 WT strain [31] and homozygous
226 $UPC2_{G648D}$ mutant strain was determined as described previously. Relative survival compared to
227 SC5314 was calculated. The homozygous $UPC2_{G648D}$ mutant strain exhibited a five-fold increase
228 in ethanol survival (**Fig. 3B**), showing that a mutation that increased ergosterol content [31] also
229 increased ethanol tolerance.

230 For a second test of the hypothesis that increased ergosterol content increases ethanol
231 tolerance, chemical stimulation of ergosterol synthesis with the anti-malarial drug artemisinin was
232 performed. Incubation of *C. albicans* with 100ug/mL of artemisinin has been shown to increase
233 ergosterol gene expression and lead to increased content of ergosterol in *C. albicans* cells [32].
234 Therefore, *C. albicans* cells were pretreated with 100ug/mL of artemisinin in DMSO or DMSO
235 alone for four hours. Artemisinin or vehicle exposure was continued during the four-hour ethanol
236 survival experiment. Survival of cells relative to SC5314 with vehicle was calculated (**Fig. 3C**).
237 Stimulation of ergosterol synthesis with artemisinin led to a 2-fold increased ethanol survival.
238 Therefore, cells with increased ergosterol content produced in several ways showed increased
239 ethanol tolerance. Increased ethanol tolerance in Esc7 is likely due, at least in part, to increased
240 ergosterol content in Esc7 cells.

241 **Altered gene expression in Esc strains**

242 We next investigated gene expression differences between Esc7 and SC5314 during
243 growth in medium A with ethanol versus medium A with water. SC5314 and Esc7 were cultured
244 in 10% EtOH medium or 10% water medium for 4 hours and RT-qPCR was used to measure
245 gene expression. We analyzed expression of genes of the ergosterol biosynthetic pathway that
246 comprise roughly half of the biosynthetic pathway from lanosterol demethylation through
247 ergosterol production [33] including *ERG11, ERG2, ERG4, ERG5, ERG6,* and *ERG25.* These
248 genes were shown to have higher transcript abundance in Esc7 in comparison to SC5314 in 10%
249 ethanol **(Fig. 4A)**. Many of these genes were repressed in ethanol in SC5314 and less repressed
250 in Esc7 in ethanol. These results were consistent with the increased concentrations of ergosterol
251 in Esc7 compared to SC5314 since increased expression of *ERG11* was shown to increase
252 ergosterol content in *C. albicans* [33].

253 **Figure 4: Differential gene expression in Esc7 versus SC5314 with and without**
254 **ethanol.** 8 biological replicate cultures were grown for 4 hours in medium A with 10% ethanol or
255 water. Gene expression was measured by RT-qPCR. Expression was normalized to expression

256 of *SPL1* (tRNA splicing gene that had unchanged expression in all conditions). Genes are
257 indicated on the x-axis and Log_2-fold change in expression is shown relative to SC5314 in 10%
258 water on the y-axis. **A)** Genes of the ergosterol pathway. **B)** Genes/pathways implicated in *S.*
259 *cerevisiae* ethanol tolerance. **C)** Genes in the ethanol catabolic pathway. Each symbol shows
260 results from an individual culture, error bars show standard deviation, and statistical significance
261 for each of the RT-qPCR figures was tested by Fisher's LSD test. Only significant differences
262 within one variable comparisons are shown. (*, $p< 0.455$, **, $p< 0.0063$, ***, $p< 0.0004$, ****, $p<$
263 0.0001)

264 Ethanol exposure has multiple effects that promote cell death including targeting the
265 membrane, and producing protein misfolding, mitochondrial stress, and DNA damage [34–36]. In
266 *S. cerevisiae,* increased expression of drug transporters and efflux pumps confers increased
267 ethanol tolerance [37,38] and we confirmed upregulation of *CDR1* in SC5314 and Esc7 during
268 exposure to ethanol as well as a trend towards greater expression in Esc7 compared to SC5314
269 (SC5314 vs Esc7 EtOH p-value: 0.2070, Fisher's LSD test, mean value 1.51-fold higher) (**Fig.**
270 **4B)**. Orthologs of genes involved in trehalose synthesis and ethanol tolerance in *S. cerevisiae,*
271 *TPS1* and *TPS2* [18], were less repressed in Esc7 compared to SC5314 in 10% EtOH (**Fig. 4B**).
272 Heat shock proteins (HSPs) and molecular chaperones are important for *S. cerevisiae*
273 ethanol tolerance [39–41]. Interestingly, *HSP90* was significantly repressed in Esc7 in ethanol
274 and was more repressed than in SC5314 (**Fig. 4B**). HSP90 is critical to many different stress
275 responses, regulates Upc2 (a transcriptional regulator of ergosterol metabolism), and regulates
276 antifungal resistance and tolerance [42–48]. Decreased expression of *HSP90* could lead to less
277 programmed cell death during ethanol stress as has been observed with exposure to hydrogen
278 peroxide [49].
279 Another pathway of interest is the ethanol catabolic pathway. This pathway has not been
280 extensively studied in *C. albicans,* however, and some of the main players in this pathway were

281 identified based on homology. Adh1 and Adh2 are thought to convert ethanol into acetaldehyde,
282 Ald4 and Ald5 likely convert acetaldehyde into acetate, and Acs1 and Acs2 likely convert acetate
283 into acetyl-CoA [50]. Several of the genes, e.g. *ADH2*, *ADH3*, *ADH4*, and *ALD5* were
284 transcriptionally induced in ethanol in both SC5314 and Esc7 **(Fig. 4C**). Significant differences in
285 expression of these genes between Esc7 and SC5314 were not observed by RT-qPCR.

286 A second approach to detect changes in gene expression that could contribute to ethanol
287 tolerance, was through RNA-sequencing. Three biological replicates of SC5314 and Esc6, 7 and
288 8 were cultured in medium A with 10% ethanol or 10% water and harvested. RNA-seq was
289 performed on RNA extracted from these samples as described in Materials and Methods and
290 results are presented in **Supplemental Tables S1-S10**. Principal coordinate analysis showed
291 that all Esc strains exhibited distinct transcriptional profiles in ethanol compared to SC5314 in
292 ethanol (**Supplemental Fig. S4**). Interestingly, *ACE2* was the most reduced transcript in Esc7
293 compared to SC5314 in 10% ethanol and was 11.3 and 4.3 fold less abundant in Esc6 and Esc8
294 in ethanol compared to SC5314 in ethanol respectively, consistent with the elevated ethanol
295 tolerance of the *ace2* deletion mutant (**Fig. 2**).

296 To determine what cellular pathways were altered in these strains, GO term analyses
297 using the Candida Genome Database (CGD) were performed as previously described [51] to
298 identify enriched categories of genes. Genes that were significantly up-regulated (log2-fold
299 change >0.5 and adjusted p-value < 0.05) in Esc strains in ethanol compared to SC5314 in
300 ethanol were analyzed (1700 genes in Esc6, 1334 genes in Esc7, and 1494 genes in Esc8). The
301 top 20 processes based on corrected p-value identified by GO term process analysis are shown
302 in **Supplemental Fig. S5**. Organonitrogen compound catabolic process was the only process that
303 was shared in the top 20 for all strains.

304 For Esc7, processes involved with ergosterol biosynthesis (red arrows in **Fig. 5**) were
305 enriched among the top 20 GO term processes, consistent with the analysis above. Esc6 and
306 Esc8 showed other enriched pathways that could be involved in ethanol tolerance or response to

307 ethanol exposure. Both Esc6 and Esc8 showed enrichment of genes involved with general
308 catabolic processes. Both strains showed enrichment of processes pertaining to proteolysis and
309 protein catabolism which could be involved with the denatured protein response caused by
310 ethanol exposure. Esc6 also showed an enrichment of genes involved with autophagy, which has
311 previously been implicated in the ethanol response of *S.* cerevisiae [52]. These findings suggest
312 that changes to proteasomal degradation/proteolysis and autophagy could contribute to ethanol
313 tolerance of *C. albicans*.

314 **Figure 5: Differential gene expression in Esc7 versus SC5314 in 10% Ethanol**.
315 Transcripts expressed more highly in Esc7 in 10% ethanol compared to SC5314 were analyzed
316 using GO term search on Candida Genome Database. Enriched processes are listed. The X
317 axis shows corrected p-value for the top 20 hits (from most significant at top and descending
318 statistical significance moving to the bottom) (triangles). Red arrows indicate processes related
319 to lipid or ergosterol synthesis.

320 These findings highlight that many pathways are likely involved in ethanol tolerance in *C.*
321 *albicans.* Some of the pathways involved in *S. cerevisiae* ethanol tolerance may not play a role in
322 the strains described here (e.g. HSPs, ethanol catabolic pathway, etc.), although genes that do
323 not change transcriptionally may also be regulated post-transcriptionally.

324

325 **<u>Esc strains show chromosome copy number variation and genomic polymorphisms</u>**

326 Whole-genome sequencing of parental SC5314, Esc6, Esc7 and Esc8 was conducted to
327 identify possible chromosome copy number variation or sequence polymorphisms in the ethanol
328 tolerant strains. Aneuploidy is a well described mechanism of stress adaptation in *C. albicans*
329 [53–55], as well as *S. cerevisiae* ethanol tolerance [56]. Genomic DNA from the strains was
330 isolated and genome sequencing was conducted by Seq-Center (formerly MiGS) using paired-

331 end Illumina next generation sequencing. Further details on sequencing and analysis workflow
332 are described in Materials and Methods.

333 Changes in chromosome copy number were detected by uploading fastq files to the Yeast
334 Mapping Analysis Pipeline (YMAP) [57]. YMAP analyzed average read depth across all
335 chromosomes to give a read-depth based chromosome copy number estimation (**Fig. 6**). These
336 images also give predictions for loss of heterozygosity (LoH) regions and show which regions are
337 predicted to be composed of which alleles (A or B, AAB or ABB in trisomic regions) based on
338 sequence homology to either of these alleles. Results show that Esc strains contain various
339 aneuploidies, as well as certain LoH regions. Specifically, Esc6 has a trisomy of Chr1, Esc7 has
340 a trisomy of Chr3, and a loss of the B allele of the short arm of chromosome R. Esc8 has a
341 monosomy of Chr5 (only A allele) and trisomies of Chr6, 7, and 8. Growth in ethanol may select
342 for aneuploid strains previously existing in the population or the presence of ethanol or byproducts
343 of its catabolism may stimulate chromosomal instability.

344 **Figure 6: Chromosome copy numbers in Esc strains.** Whole genome sequencing of
345 SC5314, Esc6, 7, and 8 was conducted as described in Materials and Methods. Copy number
346 estimates were determined based on read depth and estimated copy number is plotted along
347 chromosomes using YMAP[57]. C. albicans is diploid so euploid chromosomes show an
348 average copy number of 2 on the Y-axis as shown for SC5314. Thick black bars denote
349 aneuploidies, shown by predicted copy number greater than or less than 2. Images from YMAP
350 [57].

351 Additionally, we observed single nucleotide polymorphisms (SNPs) and
352 insertions/deletions in the genome sequences of Esc6, Esc7, and Esc8 (**supplemental tables**
353 **S11-S13**). There were 124 (in 64 different ORFs), 139 (in 83 different ORFs), and 135 (in 72
354 different ORFs) polymorphisms in protein coding regions in Esc6, Esc7, and Esc8 respectively.
355 Polymorphisms were comprised mostly of putative heterozygous polymorphisms in all strains

356 based on the allele depth ratio between the reference and alternate alleles. Heterozygous and
357 homozygous polymorphisms were classified by creating a histogram of allele depth and
358 calculating minima of a trimodal fit curve (minima = Esc6:0.1845,**0.8482**; Esc7:0.1753,**0.8716**;
359 Esc8:0.1761,**0.8628**) (**Supplemental Fig. S6**). Further analysis focused on homozygous
360 polymorphisms classified as variant calls with an allele depth ratio greater than the highest
361 minimum value (bolded values above). Only one gene carried a homozygous polymorphism in all
362 three Esc strains: *C6_02290C*, an uncharacterized gene containing a putative zinc binding
363 domain. Other genes of interest with homozygous polymorphisms are *C4_04190C* and
364 *C4_04200C* which are overlapping ORFs that both contain a putative acetyltransferase domain
365 and *PDC2* which was polymorphic in two strains. *PDC2* encodes a homeodomain-containing
366 transcriptional regulator which is involved in glucose metabolism [58]. The role of these genes in
367 ethanol tolerance is unknown.
368

369 **Esc strains exhibit reduced susceptibility to fluconazole**

370 Some of the chromosome aneuploidies observed in Esc7 and Esc8 have been previously
371 observed in strains with altered susceptibility to the frontline antifungal fluconazole. Aneuploidies
372 of chromosome 3, 5, 6, 7, and R have been implicated in azole resistance and tolerance [59–64].
373 Further, the ergosterol pathway, more specifically *ERG11,* is the target of azole class antifungals
374 and increased expression of *ERG11* and *CDR1* confers fluconazole resistance [42,65–67].

375 We therefore examined the susceptibility of Esc strains to fluconazole and other antifungal
376 drugs. Broth-microdilution assays were carried out using the standard CLSI protocol [68]. After
377 24-hour incubations, metabolic activity of the wells was measured with 2,3-bis(2-methoxy-4-nitro-
378 5-sulfophenyl)-5-[(phenylamino)carbonyl]-2H-tetrazolium hydroxide (XTT) and MIC50 and MIC70
379 values were calculated as described in Materials and Methods (**Fig. 7A**, **Supplemental Fig. S7)**.
380 Esc6 and Esc7 both exhibited fluconazole resistance phenotypes with elevated MIC50 values.
381 Esc8 showed no alterations to MIC50 values but had increased MIC70 and trailing growth,

382 suggesting altered fluconazole susceptibility. For amphotericin B and caspofungin, MICs were
383 determined by visual determination of growth and all strains showed no changes in susceptibility
384 to these antifungals (**Fig. 7C**).

385 **Figure 7: Esc strains exhibit altered fluconazole susceptibility**. **A)** Strains were
386 grown in liquid cultures containing increasing concentrations of fluconazole as described in
387 Materials and Methods. Growth was detected after a 24 hour incubation using the XTT assay for
388 metabolic activity. Metabolic activity relative to the 0ug/mL well is shown as a heat map. Yellow
389 dots show the well that corresponds to MIC70 and green dots show MIC50. Median metabolic
390 activity values from 6 biological replicates performed in 6 separate experiments are shown. **B)**
391 Strains were grown to post exponential phase in YPD liquid and then used to seed the disk
392 diffusion plates. Disk diffusion assays were performed on YPD agar with 10^5 cells/plate with
393 25ug fluconazole disks incubated for 48 hours at 30ºC. Images were taken using a Syngene
394 Imager. Representative images from an experiment repeated 4 times are shown. **C)** MIC values
395 were determined using the same MIC protocol except MICs were determined by eye. The
396 caspofungin MIC was determined from the mean of 4 biological replicate experiments for each
397 strain and the amphotericin B MIC was determined from 3 biological replicate experiments.
398 There were no significant differences between SC5314 and any of the Esc strains (testing for
399 statistical significance performed on log-transformed data, Kruskal-Wallis test for caspofungin
400 and One-Way ANOVA for amphotericin B with multiple comparisons for each)

401 Disk diffusion assays were performed following standard protocols with 25ug-loaded
402 fluconazole filter disks [69,70]. Esc7 showed no zone of inhibition following a 48-hour incubation,
403 while Esc8 showed a zone of inhibition with heavy growth within the zone (**Fig. 7B**). These
404 phenotypes were similar for voriconazole, another azole antifungal drug (**Supplemental Fig. S8**).
405 Esc7 showed no zone of voriconazole inhibition and Esc8 showed a zone of inhibition with heavy
406 growth in the zone. These results are consistent with azole resistance and azole tolerance

407 respectively. Interestingly, Esc6 showed a larger zone of fluconazole inhibition than SC5314 in
408 the disk-diffusion assay but exhibited an elevated MIC for fluconazole in the broth microdilution
409 assay. This type of discrepancy has been observed rarely and could suggest a non-canonical
410 mechanism of reduced fluconazole susceptibility in this strain. In summary, all Esc strains tested
411 exhibited altered susceptibility to fluconazole, showing that *C. albicans* can evolve fluconazole
412 resistance and tolerance through ethanol exposure without previous exposure to antifungal drugs.

413 Due to this cross-tolerance/resistance, we compared the SNPs identified in Esc strains
414 with SNPs previously identified in strains developing fluconazole resistance. Whole genome
415 sequencing analysis of strains acquired by sequentially sampling patients during the acquisition
416 of fluconazole resistance was reported by Ford, et al [69]. In this study, sequential isolates from
417 patients with *C. albicans* oral candidiasis infections were obtained. In total 43 isolates from 11
418 patients were whole-genome sequenced. 7 of the 11 patients carried fluconazole resistant strains.
419 Genome sequences and SNPs of these strains were analyzed throughout the sequential
420 isolations and compared to SC5314 reference strains. From this study, 240 genes were observed
421 with persistent polymorphisms, defined as polymorphisms observed in fluconazole resistant
422 strains from at least 3 of the 7 patients, that were nonsynonymous, were not within a region of the
423 genome with a loss of heterozygosity event and, after arising, were found in all subsequent
424 isolates.

425 We determined how many of these 240 genes carried homozygous polymorphisms in
426 Esc6, Esc7, and Esc8. There were 8 total homozygous SNP-carrying genes in Esc6 and 5 of
427 these 8 polymorphic genes also carried persistent polymorphisms in strains analyzed by Ford et
428 al. Of the 6 homozygous polymorphic genes in Esc7, 2 of these also carried persistent
429 polymorphisms in the Ford, et al strains. Esc8 had 5 homozygous polymorphic genes of which 3
430 carried persistent polymorphisms in the Ford, et al strains. This overlap in genes was greater than
431 expected by chance (p-values all < 0.0030; Chi-squared test). Genes that carry SNPs in Esc
432 strains and Ford strains are shown in **Table 1**. All polymorphisms can be found in **supplemental**

433 **tables S11-S13.** These results suggest an overlap in the selective pressures exerted by
434 fluconazole and ethanol such that these two pressures select for similar mutational landscapes
435 and aneuploidies. The similarities increase the likelihood that strains selected for higher ethanol
436 tolerance will exhibit cross-tolerance/resistance to fluconazole.

437 **Table 1*:* Polymorphic genes in Esc strains show overlap with genes associated with**
438 **fluconazole resistance***.*

Strain	**Observed Number of Common Genes[a]**	**Expected Number of Common Genes[b]**	**Two-tailed P-value (Chi squared)**
Esc6	5	0.3096	<0.0001
Esc7	2	0.2322	0.0029
Esc8	3	0.1935	<0.0001
	Homozygous Polymorphic Genes in Esc Strains		
Esc6	*ALS3, EAP1, GZF3, RFG1, TBF1, C6_04190C, C7_01100C, CR_02930W*		
Esc7	*PDC2, C1_14630C, C1_07690C, C4_04190C, C4_04200C, C6_04190C*		
Esc8	*FMO2, PDC2, PGA55, C6_03520C, C6_04190C*		
	Common Genes with Homozygous Polymorphisms in Esc strains and Persistent Polymorphisms in Ford, 2015		
Esc6	***C6_04190C,*** *TBF1, CR_02930W, ALS3, EAP1*		
Esc7	***C6_04190C,*** *C1_07690C*		
Esc8	***C6_04190C,*** *PGA55, FMO2*		

439

440 [a]240 previously identified open reading frames with persistent polymorphisms from Ford, et al,
441 2015 were compared with homozygous polymorphic open reading frames in Esc6, Esc7, and
442 Esc8. The number of common open reading frames is listed for each strain.

443 [b]The frequencies of previously identified open reading frames with persistent polymorphisms
444 from Ford, et al, 2015 and homozygous polymorphic open reading frames in Esc6, Esc7, and
445 Esc8 were used to calculate the expected number of genes in common between these 2 gene
446 sets.

447

448

449

450 **Discussion**

451 In this study, we showed that repeated exposure of *C. albicans* cultures to ethanol
452 results in selection for *C. albicans* small colony variants. The small colony variants that were
453 studied exhibited increased ethanol tolerance as measured after a four-hour ethanol exposure
454 and a longer term 24-hour ethanol exposure. Interestingly, Esc strains appeared to grow during
455 the initial hours of the ethanol exposure and then lost viability at a similar rate to SC5314. This
456 observation suggests that the evolved tolerance strategies in Esc strains were optimized for
457 short ethanol exposures consistent with the four-hour exposures that were used during the
458 selection. These mechanisms did not appear to provide much advantage during longer
459 exposure times (i.e. 8-24 hours) as the rate of optical density decay was similar in SC5314 and
460 all Esc strains in this time frame.

461 Little is known about how *C. albicans* responds to ethanol. A screen of homozygous
462 transcription factor deletion strains supported the hypothesis that the ergosterol pathway is an
463 important pathway that can impact ethanol survival in *C. albicans*. In general, ethanol kills cells
464 through disruption of the lipid bilayer [71,72], protein denaturation [73], and intracellular
465 membrane perturbations [74]. There is thinning of the bilayer through direct interdigitation of
466 ethanol between membrane lipids, and ultimately denaturation of the membrane which will
467 result in cell death [71,72]. We showed here that increased ergosterol content in *C. albicans* can
468 confer increased ethanol survival. This is likely due to protection from the impacts of ethanol
469 perturbation on the plasma membrane. Models of yeast plasma membranes showed that
470 increased ergosterol content in the membrane reduced ethanol interdigitation and contributed to
471 resistance against the membrane thinning effect of ethanol [72,75].

472 We asked whether *UPC2* was involved in the differential expression of *ERG* genes as
473 Upc2 is a global regulator of ergosterol biosynthesis [76]. However, *UPC2* expression was
474 decreased in Esc7 in 10% ethanol compared to SC5314 (**supplemental table S3**), and there
475 were no SNPs in the *UPC2* orf or promoter sequence, suggesting that other novel

476 transcriptional regulators of ergosterol synthesis are regulating *ERG* gene expression in Esc7.
477 Additionally, post-transcriptional regulatory mechanisms could lead to greater activation of
478 Upc2. For example in *S. cerevisiae* and *Candida* species, it has been suggested that HSP90
479 acts as a pedestal for Upc2 and binds it in an inactive form [77,78]. It is possible that similar
480 mechanisms are at play in *C. albicans.* In Esc7, there is a higher ratio of *UPC2*/*HSP90*
481 transcripts in Esc7 in 10% ethanol compared to SC5314 in 10% ethanol based on the RNA-Seq
482 data (**Supplemental Fig. S9**). Regulation of the *UPC2/HSP90* ratio could lead to a greater
483 proportion of Upc2 being in its active form, thus leading to greater ergosterol production.
484 Furthermore, another transcriptional regulator of ergosterol gene expression, *ADR1* [79], also
485 had no polymorphisms in any of the Esc strains.

486 Multiple mechanisms including lipid metabolism alterations, aneuploidy, increased
487 production of stress responsive genes, and drug efflux pump expression have all been shown to
488 confer greater ethanol tolerance in *S. cerevisiae* [18,56,80]. We hypothesized that *C. albicans*
489 utilizes multiple mechanisms to increase ethanol tolerance and improve survival when exposed
490 to relatively high concentrations of ethanol. Ethanol affects many different pathways in cells
491 such as protein folding, lipid bilayer integrity, and mitochondrial and nuclear function [71–74,81].
492 In *C. albicans* specifically, ethanol also affects filamentation and biofilm formation [82].
493 Therefore, many different pathways are under selection during repeated exposure to ethanol
494 and roughly 44% of all genes showed statistically significant alterations in gene expression in
495 the 10% ethanol comparison of Esc7 and SC5314 (**supplemental table S3**). These large
496 transcriptomic changes in Esc strains in ethanol indicate that many *C. albicans* pathways are
497 likely impacted during ethanol exposure. The transcription factor deletion strains with altered
498 ethanol tolerance affected many pathways and processes including biofilm formation, regulation
499 of filamentation, cell-cell adhesion, and cell wall synthesis.

500 The Esc strains showed reduced susceptibility to the antifungal drug fluconazole and
501 voriconazole but not to other antifungals. These observations suggest that at least part of the

502 overlap of selective pressures between fluconazole and ethanol revolves around ergosterol. If a
503 stressor impacts a pathway that an antifungal drug also targets, the stressor could theoretically
504 select for drug resistant or tolerant strains. Even if there is no overlap in the phenotypic response
505 to a stimulus and an antifungal, if the resistance mechanism involves aneuploidy, cross-resistance
506 could arise due to increased dosage of genes. Previously this has been shown in *C. albicans* with
507 pre-exposure to chemotherapeutic drugs leading to decreased caspofungin susceptibility [64].
508 We show similar but novel findings—*C. albicans* can evolve fluconazole resistance and higher
509 tolerance after repeated exposure to a naturally occurring molecule, ethanol.

510 An unusual fluconazole resistance phenotype was observed for Esc6, defined as a
511 susceptible disk-diffusion phenotype and a strong resistance phenotype observed by broth-
512 microdilution. There have been well documented discrepancies between broth-microdilution
513 assays and disk-diffusions [83]. However, discrepancies to the degree that we observed with Esc6
514 are uncommon. These observations suggest that Esc6 has developed a noncanonical
515 mechanism of resistance, or that Esc6 shows an environment-dependent mechanism of
516 resistance. Recently it has been shown that large discrepancies in susceptibility of vulvovaginal
517 candidiasis (VVC) isolates to fluconazole can be observed in clinical testing laboratories
518 depending on the pH of testing media. A pH of 4.5, which more accurately represents the pH of
519 the vagina, is more likely to identify a VVC strain as resistant than pH 7. Testing at pH 4.5 more
520 accurately explained treatment recalcitrance than susceptibilities obtained from testing at pH 7
521 [84]. Further studies of Esc6 will be needed to identify the basis for its fluconazole phenotypes.

522 Esc7 showed genetic alterations previously identified in fluconazole resistant strains
523 including Chr3 trisomy [59–61] and higher expression of genes in the ergosterol pathway. These
524 genetic changes have previously been implicated in fluconazole resistance [57–59]. However,
525 Esc7 did not show large changes to *CDR1*, *CDR2*, or *MDR1* expression in the conditions we
526 examined. Previously this was thought to be part of the mechanism of fluconazole resistance in
527 strains with Chr3 trisomies as *CDR1, CDR2,* and *MRR1* reside on Chr3 [59,85].

528 Aneuploidies found in Esc8 included a monosomy of Chr5, and trisomies of Chr6, Chr7,
529 and ChrR. ChrR trisomy has been found in fluconazole tolerant strains and shown to confer
530 increased fluconazole tolerance [62–64]. Aneuploidies may contribute to the reduced fluconazole
531 susceptibility of Esc8.

532 Aneuploidies, while likely part of the resistance and tolerance mechanisms of these
533 strains, are not the only interesting genomic changes. Esc strains also carry SNPs in genes that
534 were altered during the acquisition of fluconazole resistance in clinical isolates [69]. Likely, some
535 of these SNPs confer a fitness advantage for Esc strains during growth in fluconazole. One of
536 these polymorphic genes of interest is *C6_04190C* which encodes an uncharacterized orf with a
537 putative zinc binding domain. *C6_04190C* was polymorphic in all Esc strains as well as the Ford,
538 et al strains. Perhaps C6_04190C plays a role in zinc uptake or zinc sequestration, which could
539 affect zinc-binding transcriptional regulators that are involved with fluconazole resistance such as
540 Mrr1, Mrr2, Tac1, and Upc2 [86–88]. Modifying the pool of biologically available zinc could affect
541 the activity of these various proteins and have effects on susceptibility to fluconazole.

542 In summary, we have shown that *C. albicans* can evolve increased ethanol tolerance
543 following repeated exposure to ethanol. This is likely due to the involvement of many different
544 pathways. Repeated ethanol exposure selects for Esc strains that have altered transcriptional
545 responses to ethanol and altered genomic structure. We also showed that increased ergosterol
546 content leads to enhanced ethanol survival. The mutational landscape of *C. albicans* Esc strains
547 resembles the landscape of genes mutated in clinical isolates upon acquisition of fluconazole
548 resistance. This finding highlights the overlap of selective pressures between the two stressors:
549 fluconazole and ethanol. Consistent with this overlap, we demonstrated that strains repeatedly
550 exposed to ethanol acquire fluconazole resistance and tolerance without previous exposure to
551 antifungal drugs.

552

553 **Materials and Methods**

554

555 **Strains and Culture Conditions**

556 For the repeated ethanol exposure protocol, individual colonies of *C. albicans* strain
557 SC5314 were inoculated into 10 mL of YPD and grown overnight at 30ºC to post exponential
558 phase (16-20 hours). 5 independent cultures were split into paired cultures to be exposed to media
559 with ethanol or water. After overnight growth, cells were washed with PBS, counted on a
560 hemocytometer and 10^6 cells were inoculated from the overnight YPD cultures into 1 mL of
561 medium A (Dulbecco's Modified Eagle Medium (DMEM) with 10% fetal bovine serum and 1X non-
562 essential amino acids) with ethanol or water in 2 mL screw cap microcentrifuge tubes. The
563 concentrations of ethanol or water were 1% for the first exposure, 2% for the second exposure,
564 4% for the third exposure, 6% for the fourth exposure, 8% for the fifth exposure, and 10% for
565 exposures six through eight (volume/volume). Cultures were incubated at 37ºC in a 5% CO_2
566 atmosphere for four hours to mimic physiological conditions. Following ethanol or water exposure,
567 10 uL of the medium A cultures were seeded into 10 mL YPD for recovery from the ethanol
568 exposure and grown at 30ºC until post-exponential phases were reached (1 day for passages in
569 6% ethanol or less or 2 days for passages in 8% and 10% ethanol). 100 uL of each population
570 was plated on YPD agar and incubated for 2 days at 30ºC following each medium A exposure to
571 monitor population dynamics and normal sized and small sized colonies were counted by eye.
572 Small colonies were defined as colonies estimated to be 50% or less in size compared to normal
573 sized colonies.

574 Ethanol small colony (Esc) strains were isolated from different populations of cells at
575 different time points in the repeated ethanol exposure protocol by picking colonies from the YPD
576 agar plates. Populations 1-4 were populations repeatedly exposed to water and 5-8 were
577 populations repeatedly exposed to ethanol. Esc6 was isolated from population 8 in the 6th passage
578 in ethanol (first exposure to 10% ethanol), Esc7 was isolated from population 6 in the 7th passage
579 in ethanol (second exposure to 10% ethanol), and Esc8 was isolated from the 5th population in

580 the 8th passage in ethanol (third exposure to 10% ethanol). SC5314-UPC2-G648D was obtained
581 from Dr. Joachim Morschhauser and has the following genotype: *UPC2-G648D::FRT/UPC2-*
582 *G648D::FRT* [31].
583 For the ethanol screen with strains from the Homann collection [17], strains were obtained
584 in a 96-well format from the Fungal Genetics Stock Center. Strains were then isolated from the
585 96 well plates and struck for isolation on YPD-agar plates. Individual colonies were isolated for
586 each strain, and grown for 20 hours to post-exponential phase before use in the screen. The
587 screen followed the same four-hour ethanol exposure protocol as described above.
588
589 **Ethanol Exposure to Test for Ethanol Survival**
590 Strains were grown to post-exponential phase in YPD (16-20 hours) and then counted
591 using a hemocytometer to seed 10^6 cells in one mL of medium A with 10% H2O or 10% ethanol
592 (vol/vol) using 95% ethanol in 2 mL screw cap tubes. Cultures were incubated for 4 hours in 37ºC
593 in a 5% CO_2 atmosphere. Before incubation, 100 uL was sampled from the cultures and serially
594 diluted onto YPD-agar plates for a starting CFU determination. Following 4 hours, cultures were
595 sampled and diluted serially in 1X phosphate-buffered saline (PBS) and plated on YPD agar for
596 a final CFU determination for the water and ethanol cultures. YPD-agar plates were incubated for
597 2 days at 30ºC and counted. The final CFU from the ethanol cultures was divided by the final CFU
598 from the water cultures to determine percentage survival and then calculated as a survival relative
599 to SC5314 within each separate experiment. For the screen of transcription factor deletion
600 mutants, these strains were compared to their parent strain, SN152, for a determination of relative
601 survival.
602 For the extended incubation, the same conditions were used as above except cultures
603 were incubated in 37ºC incubators with ambient CO_2 concentrations. Two separate cultures for
604 each biological replicate were set up for each individual experiment. The first set of cultures was

605 sampled at 0, 2, 4, and 6 hours and the second set was sampled at 8, 10, 12, and 24 hours.
606 Survival was calculated relative to starting CFU obtained at timepoint 0 hours.
607
608 **RNA isolation, RT-qPCR, and RNA-sequencing**
609 Cultures of SC5314 or Esc strains were grown to post-exponential phase and 10^8 cells for
610 each were seeded into 1 mL cultures of medium A with 10% H_2O or EtOH and incubated for 4
611 hours at 37ºC with 5% CO_2. Immediately following the incubation, cells were centrifuged at 6000
612 rpm for 1 min and supernatant was removed. Cells were then resuspended in 1 mL of RNA-later
613 (Fisher cat. AM7021) and immediately frozen at -80ºC. Cells were thawed on ice and lysed as
614 previously described by bead-beating [89]. RNA was isolated using the Invitrogen Purelink RNA
615 mini kit (Thermo Fisher cat: 12183-025) with the on-column DNase treatment (Thermo Fisher cat:
616 12185-010). RNA was eluted in 40uL of ultrapure H_2O and RNA yield and purity were assessed
617 on a Nanodrop.
618 For RT-qPCR, cDNA was synthesized using SSIII reverse transcriptase (Thermo cat:
619 18080-085) following manufacturer's protocol with approximately 1 ug starting RNA
620 concentrations. Oligo-dT primers were used for each cDNA synthesis reaction. Eight biological
621 replicates for each strain and condition were used. cDNA was diluted 1:5 in ultrapure H_2O and 1
622 uL was used per reaction for RT-qPCR. SYBR green master mix (Fisher cat: 4334973) was used
623 and qPCR reactions were run on a Roche Lightcycler 480 II using standard two-step reaction
624 procedures. Controls without cDNA were run for each primer and all primer pairs either did not
625 yield product, or yielded Cp values that were at least 10 cycles greater than the sample Cp value.
626 Melting curves were analyzed to ensure only one peak was seen and primer dimerization was not
627 observed in any of the curves analyzed. Cp values were normalized using *SPL1*, encoding a tRNA
628 splicing enzyme that showed no significant changes in gene expression in all conditions. The fold
629 change in gene expression relative to SC5314 in 10% H2O was then calculated and graphed by
630 $2^{-\Delta\Delta CT}$ values [90]. Primers are shown in **supplemental table S14**. Primer sequences were either

631 used from previously published work or were designed using NCBI primer blast. Primer design
632 used the A allele sequence of the target gene, *C. albicans* strain SC5314 reference genome, PCR
633 product size of 90-250bp, optimized primer length of 28 nucleotides, primer melting temperatures
634 of 53-63ºC with 56ºC optimized temperature and a max primer pair difference of 5ºC. Purified
635 PCR products were sequenced to verify target specificity.

636 For RNA-seq, three biological replicates of SC5314, Esc6, Esc7, or Esc8 following
637 exposure to medium A with 10% water or 10% EtOH were sent for sequencing. All samples
638 sequenced had RNA integrity scores of 9.2 or greater. cDNA libraries were made by Genewiz
639 and RNA-seq was performed by Genewiz as previously described [70] with the following
640 alterations: gene expression was considered significant only if adjusted-P-value (calculated by
641 Benjamini-Hochberg test) was less than 0.05 and $\log_2$-fold change was greater than the absolute
642 value of 0.5. RNA-sequencing was aligned to *Candida albicans* SC5314 (assembly ASM18296v3)
643 as the reference genome. Gene ontology of significant hits were assessed using Candida
644 Genome Database Go term finder as has been previously described [51]
645 (http://candidagenome.org). For gene expression differences, the three biological replicates from
646 each condition were averaged and significant differences were compared by relative transcript
647 abundance differences.

648

649 **Ergosterol Quantitation**

650 Total cellular ergosterol was quantitated as described previously [27,29,30]. 10^8 cells of
651 SC5314 or Esc strains were incubated for 4 hours at 37ºC with 5% CO_2 in medium A with 10%
652 ethanol or 10% H_2O. After the four-hour incubation, cells were pelleted and washed twice in sterile
653 PBS. Following washing, supernatant was removed, and the wet pellet weight of the cells was
654 measured. 2 mL of alcoholic 25% potassium hydroxide was added to each tube for saponification
655 and pellets were resuspended by vortexing for 1 min, transferred to borosilicate glass tubes, and
656 incubated in an 85ºC water bath for 1 hour. Following the incubation, tubes were allowed to cool

657 for 10 mins at room temperature and 2 mL of spectroscopy grade n-heptane (Sigma 1043660500)
658 and 667 uL of sterile deionized water were added to each tube and vortexed for 3 mins. The
659 organic fraction was removed from the mixture and diluted 1:2 in 100% ethanol (Sigma cat:
660 E7023-1L). Scanning absorbance values were then taken between 230nm and 290nm on a
661 Nanodrop spectrophotometer. Calculation of the amount of ergosterol and amount of dehydro-
662 ergosterol (DHE) normalized to wet pellet weight was performed as described previously
663 [43,82,83]. In summary, the calculation was **equation 1:** % (ergosterol + DHE) = [(A_{282}/290) x
664 dilution factor] / pellet weight. **Equation 2:** % DHE = [(A_{230}/518) x dilution factor]/pellet weight. %
665 ergosterol = **Equation 1 – Equation 2**. The dilution factor is the dilution factor used for diluting
666 the sterol-containing heptane solution with ethanol, 290 = E for ergosterol at 282 nm, and 518 =
667 E for DHE at 230 nm [27].
668
669
670 **Whole-Genome Sequencing**
671 Genomic DNA from SC5314 and Esc strains was extracted and sent to SeqCenter for
672 next-generation sequencing. SC5314 and Esc6 yielded consistent colony sizes so these strains
673 were struck out on YPD-agar and isolated colonies were picked, grown to post-exponential phase
674 and cells were pelleted. Esc7 and Esc8 have more unstable small colony phenotypes, therefore,
675 cells were plated on a YPD-agar plate grown for 3 days at 30ºC and small colonies were picked
676 and added to 100uL of sterile PBS. This was then used to seed 4 new plates and performed three
677 separate times. The plates with the lowest reversion rates were used for genome preps by
678 collecting small colonies from these plates and adding them to 5 mL of sterile PBS. These tubes
679 were then vortexed, and cells were pelleted. Genomes were extracted using bead-beating in
680 phenol chloroform followed by chloroform extraction and ethanol precipitation as described
681 previously [91]. DNA was purified further by the Qiagen DNeasy kit using manufacturer's protocol.

682 Whole-genome sequencing was performed by SeqCenter by paired end NGS Illumina
683 sequencing of 151 bp reads. Quality control and adaptor trimming were performed with bcl-
684 convert [92], and reads were mapped to SC5314 reference genome using bwa [93]. Genome
685 coverage from the sequencing runs ranged from 66X to 83X based on total number of reads
686 across the SC5314 reference genome length. GATK's Markduplicates was used to remove
687 duplicate reads in the alignment and GATK's Haplotype caller was used to call variants in the
688 alignment [94]. Variants with a QD < 2, or MQ < 40, or MGRankSum < -12.5, or
689 ReadPosRankSum < -8, or FS > 60.0, or SOR > 3 were filtered out. Sequence variants were
690 compiled into an excel document by SeqCenter. Due to the large number of sequence variants
691 obtained, only homozygous sequence variants of Esc strains compared to the parental SC5314
692 strain sequence were analyzed in depth. Homozygous sequence variants were determined by
693 constructing a histogram of allele depth and calculating minima of a trimodal fit curve
694 (**Supplemental Fig. S6**). Homozygous polymorphisms were classified as variant calls with an
695 allele depth ratio greater than the high minima value. Heterozygous polymorphisms were
696 classified as those with allele depth ratios between the two minima values. Polymorphisms with
697 allele depth ratio lower than the high minima and less than a total read depth of 10 were excluded
698 from analysis. For the remaining putative homozygous polymorphisms, pre-existing heterozygous
699 polymorphisms in the B allele were excluded by examining the location of the polymorphism in a
700 multiple sequence alignment of the A and B alleles of the gene.

701 Chromosome copy number variations were analyzed using the Yeast Mapping Analysis
702 Pipeline [57]. Fastq files were uploaded to YMAP and YMAP calculated the average read depth
703 across the chromosomes mapping to SC5314 as the reference genome. YMAP thus generates
704 chromosome copy number predictions based on the read depth across the genome. These
705 predictions were graphed as predicted copy number across chromosomes of the individual strains
706 relative to a ploidy of 2. Changes in ploidy were shown by thick black bars deviating from the
707 starting ploidy line at 2.

708

709 **Disk-Diffusion and Broth-Microdilution Assays**

710 For the disk-diffusion assay, cells were grown to post-exponential phase in liquid YPD
711 medium and 10^5 cells per plate were spread onto YPD-agar. Then 6mm diameter Whatman #1
712 filter disks impregnated with 25ug of fluconazole or 1ug of voriconazole were placed in the center
713 of the YPD agar. These plates were incubated for 48 hours at 30ºC to assess the zone of inhibition
714 and the fraction of growth within the zone. Images of plates following incubation were taken on a
715 Syngene gel-doc imager using white light, black background, and identical iris, zoom, and focus
716 settings for each plate. Representative images of each strain are shown. Eight biological
717 replicates of each strain were tested in four different experiments for fluconazole or 6 biological
718 replicates in three different experiments for voriconazole.

719 For the broth-microdilution assay, cells were grown as stated above and 10^4 cells/well
720 were used for each strain and experiment. Standard CLSI protocol was used for this experiment.
721 Cells were diluted in RPMI, 165 mM MOPS, 2% glucose, pH 7.0. Antifungals were serially diluted
722 2-fold—yielding final concentrations from 64 ug/mL down to 0.125 ug/mL for fluconazole, 2 to
723 0.015ug/mL for caspofungin or 4 to 0.03ug/mL for amphotericin B. In each row, a no-cell well was
724 used as a blank and sterility control, and a no-drug control was used to calculate 100% metabolic
725 activity. Plates were incubated for 24 hours at 35ºC. Growth was determined by visual growth for
726 amphotericin B and caspofungin or by measurement of metabolic activity for fluconazole. For the
727 latter measurement, medium was carefully removed from each well and 100 uL of 1 mg/mL of
728 2,3-bis(2-methoxy-4-nitro-5-sulfophenyl)-5-[(phenylamino)carbonyl]-2H-tetrazolium hydroxide
729 (XTT) (Alfa-Aesar) in PBS with 4 uL of menadione per/100 uL was added to each well. The plates
730 were incubated for one hour at room temperature and then 50 uL of solution from each well was
731 removed and read at 492 nm to determine metabolic activity of each well. The no-drug well
732 averaged between the two duplicates was used to calculate the OD492 that indicates a 50%
733 reduction. The concentration of drug that yielded a reduction in metabolic activity immediately

734 less than 50% of the no-drug well was considered the MIC50. The heat map of the metabolic
735 activity of these wells is shown as the medians of 6 biological replicates for each strain in **Fig. 7**
736 or shown as individual values in **Supplemental Fig. S7**. Heat map was made using GraphPad
737 Prism.
738

739 **Author Contributions**

740 Conceptualization, A.W.D. and C.A.K.; investigation, A.W.D.; writing—original draft preparation,
741 A.W.D.; writing—review and editing, C.A.K., A.W.D.; funding acquisition, C.A.K. All authors have
742 read and agreed to the published version of the manuscript.

743 **Funding**

744 A.W.D. was supported by training grant T32AI007422 from the National Institutes of Health. This
745 research was supported by grant R01AI118898 from the National Institutes of Health (to C.A.K.).
746 The funders had no role in study design, data collection or the decision to publish the manuscript.

747 **Acknowledgements:** We thank Dr. Joachim Morschhäuser (Universität Wurzburg) for the kind
748 gift of the *UPC2*$_{G648D}$ mutant strain, Dr. Albert Tai for help with the whole-genome sequencing
749 analysis, and Drs. Jesus Romo, Paola Zucchi, and Ashlee Junier for helpful discussion. We
750 would also like to thank Jeyra Perez Lozada and Dayana Alay Gonzalez for technical
751 assistance.

752 **Data Availability Statement:** Whole-genome sequencing fastq files are available on the NCBI
753 sequence read archive (project: PRJNA1018434). Gene expression matrices are available on the
754 Genome Expression Omnibus (GEO project: GSE243757).

755

756 **References**

757 1. McCarty TP, White CM, Pappas PG. Candidemia and Invasive Candidiasis. Infect Dis Clin North Am.
758 2021 Jun;35(2):389–413.

759 2. MacCallum DM. Hosting Infection: Experimental Models to Assay *Candida* Virulence. Int J Microbiol.
760 2012;2012:1–12.

761 3. Mejia-Chew C, O'Halloran JA, Olsen MA, Stwalley D, Kronen R, Lin C, et al. Effect of infectious
762 disease consultation on mortality and treatment of patients with candida bloodstream infections: a
763 retrospective, cohort study. Lancet Infect Dis. 2019 Dec;19(12):1336–44.

764 4. Fujihara N, Saito T, Kudo T, Iinuma Y, Ichiyama S, Takakura S. Clinical factors associated with
765 fluconazole resistance and short-term survival in patients with Candida bloodstream infection. Eur J
766 Clin Microbiol Infect Dis. 2004 May 1;23(5):380–8.

767 5. Kato H, Yoshimura Y, Suido Y, Shimizu H, Ide K, Sugiyama Y, et al. Mortality and risk factor analysis
768 for Candida blood stream infection: A multicenter study. J Infect Chemother. 2019 May;25(5):341–5.

769 6. Pande K, Chen C, Noble SM. Passage through the mammalian gut triggers a phenotypic switch that
770 promotes Candida albicans commensalism. Nat Genet. 2013 Sep;45(9):1088–91.

771 7. Zhai B, Ola M, Rolling T, Tosini NL, Joshowitz S, Littmann ER, et al. High-resolution mycobiota
772 analysis reveals dynamic intestinal translocation preceding invasive candidiasis. Nat Med. 2020
773 Jan;26(1):59–64.

774 8. Kotey FC, Dayie NT, Tetteh-Uarcoo PB, Donkor ES. *Candida* Bloodstream Infections: Changes in
775 Epidemiology and Increase in Drug Resistance. Infect Dis Res Treat. 2021 Jan;14:117863372110269.

776 9. Chu H, Duan Y, Lang S, Jiang L, Wang Y, Llorente C, et al. The Candida albicans exotoxin candidalysin
777 promotes alcohol-associated liver disease. J Hepatol. 2020 Mar;72(3):391–400.

778 10. Yang AM, Inamine T, Hochrath K, Chen P, Wang L, Llorente C, et al. Intestinal fungi contribute to
779 development of alcoholic liver disease. J Clin Invest. 2017 May 22;127(7):2829–41.

780 11. Hartmann P, Lang S, Zeng S, Duan Y, Zhang X, Wang Y, et al. Dynamic Changes of the Fungal
781 Microbiome in Alcohol Use Disorder. Front Physiol. 2021 Jul 19;12:699253.

782 12. Rubbens J, Brouwers J, Wolfs K, Adams E, Tack J, Augustijns P. Ethanol concentrations in the human
783 gastrointestinal tract after intake of alcoholic beverages. Eur J Pharm Sci. 2016 Apr;86:91–5.

784 13. Halsted CH, Robles EA, Mezey E. Distribution of ethanol in the human gastrointestinal tract. Am J
785 Clin Nutr. 1973 Aug;26(8):831–4.

786 14. Stanley D, Fraser S, Chambers PJ, Rogers P, Stanley GA. Generation and characterisation of stable
787 ethanol-tolerant mutants of Saccharomyces cerevisiae. J Ind Microbiol Biotechnol. 2010
788 Feb;37(2):139–49.

789 15. Turanlı-Yıldız B, Benbadis L, Alkım C, Sezgin T, Akşit A, Gökçe A, et al. In vivo evolutionary
790 engineering for ethanol-tolerance of Saccharomyces cerevisiae haploid cells triggers diploidization. J
791 Biosci Bioeng. 2017 Sep;124(3):309–18.

792 16. Balaban NQ, Helaine S, Lewis K, Ackermann M, Aldridge B, Andersson DI, et al. Definitions and
793 guidelines for research on antibiotic persistence. Nat Rev Microbiol. 2019 Jul;17(7):441–8.

794 17. Homann OR, Dea J, Noble SM, Johnson AD. A Phenotypic Profile of the Candida albicans Regulatory
795 Network. Copenhaver GP, editor. PLoS Genet. 2009 Dec 24;5(12):e1000783.

796 18. Ma M, Liu ZL. Mechanisms of ethanol tolerance in Saccharomyces cerevisiae. Appl Microbiol
797 Biotechnol. 2010 Jul;87(3):829–45.

798 19. Arnaud MB. The Candida Genome Database (CGD), a community resource for Candida albicans gene
799 and protein information. Nucleic Acids Res. 2004 Dec 17;33(Database issue):D358–63.

800 20. Hameed S, Dhamgaye S, Singh A, Goswami SK, Prasad R. Calcineurin Signaling and Membrane Lipid
801 Homeostasis Regulates Iron Mediated MultiDrug Resistance Mechanisms in Candida albicans. Davis
802 D, editor. PLoS ONE. 2011 Apr 12;6(4):e18684.

803 21. Mulhern SM, Logue ME, Butler G. *Candida albicans* Transcription Factor Ace2 Regulates Metabolism
804 and Is Required for Filamentation in Hypoxic Conditions. Eukaryot Cell. 2006 Dec;5(12):2001–13.

805 22. Sellam A, Askew C, Epp E, Tebbji F, Mullick A, Whiteway M, et al. Role of Transcription Factor
806 CaNdt80p in Cell Separation, Hyphal Growth, and Virulence in Candida albicans. Eukaryot Cell. 2010
807 Apr;9(4):634–44.

808 23. Sellam A, Van Het Hoog M, Tebbji F, Beaurepaire C, Whiteway M, Nantel A. Modeling the
809 Transcriptional Regulatory Network That Controls the Early Hypoxic Response in Candida albicans.
810 Eukaryot Cell. 2014 May;13(5):675–90.

811 24. Shobayashi M, Mitsueda S ichiro, Ago M, Fujii T, Iwashita K, Iefuji H. Effects of Culture Conditions on
812 Ergosterol Biosynthesis by *Saccharomyces cerevisiae*. Biosci Biotechnol Biochem. 2005
813 Jan;69(12):2381–8.

814 25. del Castillo Agudo L. Lipid content of Saccharomyces cerevisiae strains with different degrees of
815 ethanol tolerance. Appl Microbiol Biotechnol. 1992 Aug;37(5):647–51.

816 26. Kubota S, Takeo I, Kume K, Kanai M, Shitamukai A, Mizunuma M, et al. Effect of Ethanol on Cell
817 Growth of Budding Yeast: Genes That Are Important for Cell Growth in the Presence of Ethanol.
818 Biosci Biotechnol Biochem. 2004 Jan;68(4):968–72.

819 27. Arthington-Skaggs BA, Jradi H, Desai T, Morrison CJ. Quantitation of Ergosterol Content: Novel
820 Method for Determination of Fluconazole Susceptibility of *Candida albicans*. J Clin Microbiol. 1999
821 Oct;37(10):3332–7.

822 28. Breivik ON, Owades JL. Yeast Analysis, Spectrophotometric Semimicrodetermination of Ergosterol in
823 Yeast. J Agric Food Chem. 1957 May;5(5):360–3.

824 29. Alizadeh F, Department of Microbiology, Yasooj Branch, Islamic Azad University, Yasooj, Iran.,
825 Khodavandi A, Department of Biology, Gachsaran Branch, Islamic Azad University, Gachsaran, Iran,
826 Zalakian S, Department of Microbiology, Yasooj Branch, Islamic Azad University, Yasooj, Iran.

827 Quantitation of ergosterol content and gene expression profile of ERG11 gene in fluconazole-
828 resistant Candida albicans. Curr Med Mycol. 2017 Mar 1;3(1):13–9.

829 30. Santos JRA, Gouveia LF, Taylor ELS, Resende-Stoianoff MA, Pianetti GA, César IC, et al. Dynamic
830 Interaction between Fluconazole and Amphotericin B against Cryptococcus gattii. Antimicrob Agents
831 Chemother. 2012 May;56(5):2553–8.

832 31. Flowers SA, Barker KS, Berkow EL, Toner G, Chadwick SG, Gygax SE, et al. Gain-of-Function
833 Mutations in *UPC2* Are a Frequent Cause of *ERG11* Upregulation in Azole-Resistant Clinical Isolates
834 of Candida albicans. Eukaryot Cell. 2012 Oct;11(10):1289–99.

835 32. Zhu C, Liao B, Ye X, Zhou Y, Chen X, Liao M, et al. Artemisinin elevates ergosterol levels of Candida
836 albicans to synergise with amphotericin B against oral candidiasis. Int J Antimicrob Agents. 2021
837 Sep;58(3):106394.

838 33. Sanglard D, Ischer F, Parkinson T, Falconer D, Bille J. *Candida albicans* Mutations in the Ergosterol
839 Biosynthetic Pathway and Resistance to Several Antifungal Agents. Antimicrob Agents Chemother.
840 2003 Aug;47(8):2404–12.

841 34. Pais TM, Foulquié-Moreno MR, Hubmann G, Duitama J, Swinnen S, Goovaerts A, et al. Comparative
842 Polygenic Analysis of Maximal Ethanol Accumulation Capacity and Tolerance to High Ethanol Levels
843 of Cell Proliferation in Yeast. Jinks-Robertson S, editor. PLoS Genet. 2013 Jun 6;9(6):e1003548.

844 35. Ibeas JI, Jimenez J. Mitochondrial DNA loss caused by ethanol in Saccharomyces flor yeasts. Appl
845 Environ Microbiol. 1997 Jan;63(1):7–12.

846 36. Snoek T, Verstrepen KJ, Voordeckers K. How do yeast cells become tolerant to high ethanol
847 concentrations? Curr Genet. 2016 Aug;62(3):475–80.

848 37. Teixeira MC, Mira NP, Sá-Correia I. A genome-wide perspective on the response and tolerance to
849 food-relevant stresses in Saccharomyces cerevisiae. Curr Opin Biotechnol. 2011 Apr;22(2):150–6.

850 38. Song Y, Li S, Zhao Y, Zhang Y, Lv Y, Jiang Y, et al. ADH1 promotes Candida albicans pathogenicity by
851 stimulating oxidative phosphorylation. Int J Med Microbiol. 2019 Sep;309(6):151330.

852 39. Piper PW, Talreja K, Panaretou B, Moradas-Ferreira P, Byrne K, Praekelt UM, et al. Induction of
853 major heat-shock proteins of Saccharomyces cerevisiae, including plasma membrane Hsp30, by
854 ethanol levels above a critical threshold. Microbiology. 1994 Nov 1;140(11):3031–8.

855 40. Ogawa Y, Nitta A, Uchiyama H, Imamura T, Shimoi H, Ito K. Tolerance mechanism of the ethanol-
856 tolerant mutant of sake yeast. J Biosci Bioeng. 2000 Jan;90(3):313–20.

857 41. McClellan AJ, Xia Y, Deutschbauer AM, Davis RW, Gerstein M, Frydman J. Diverse Cellular Functions
858 of the Hsp90 Molecular Chaperone Uncovered Using Systems Approaches. Cell. 2007
859 Oct;131(1):121–35.

860 42. Shapiro RS, Uppuluri P, Zaas AK, Collins C, Senn H, Perfect JR, et al. Hsp90 Orchestrates
861 Temperature-Dependent Candida albicans Morphogenesis via Ras1-PKA Signaling. Curr Biol. 2009
862 Apr;19(8):621–9.

863 43. Singh SD, Robbins N, Zaas AK, Schell WA, Perfect JR, Cowen LE. Hsp90 Governs Echinocandin
864 Resistance in the Pathogenic Yeast Candida albicans via Calcineurin. Mitchell AP, editor. PLoS
865 Pathog. 2009 Jul 31;5(7):e1000532.

866 44. Diezmann S, Michaut M, Shapiro RS, Bader GD, Cowen LE. Mapping the Hsp90 Genetic Interaction
867 Network in Candida albicans Reveals Environmental Contingency and Rewired Circuitry. Snyder M,
868 editor. PLoS Genet. 2012 Mar 15;8(3):e1002562.

869 45. Li C, Tu J, Han G, Liu N, Sheng C. Heat shock protein 90 (Hsp90)/Histone deacetylase (HDAC) dual
870 inhibitors for the treatment of azoles-resistant Candida albicans. Eur J Med Chem. 2022
871 Jan;227:113961.

872 46. Xu Y, Lu H, Zhu S, Li WQ, Jiang Y ying, Berman J, et al. Multifactorial Mechanisms of Tolerance to
873 Ketoconazole in Candida albicans. Cuomo CA, editor. Microbiol Spectr. 2021 Sep 3;9(1):e00321-21.

874 47. Van Hauwenhuyse F, Fiori A, Van Dijck P. Ascorbic Acid Inhibition of Candida albicans Hsp90-
875 Mediated Morphogenesis Occurs via the Transcriptional Regulator Upc2. Eukaryot Cell. 2014
876 Oct;13(10):1278–89.

877 48. Rogers PD. Sterol homeostasis in yeast. Nat Chem Biol. 2022 Nov;18(11):1170–1.

878 49. Dai B, Wang Y, Li D, Xu Y, Liang R, Zhao L, et al. Hsp90 Is Involved in Apoptosis of Candida albicans by
879 Regulating the Calcineurin-Caspase Apoptotic Pathway. Nielsen K, editor. PLoS ONE. 2012 Sep
880 18;7(9):e45109.

881 50. Nieminen MT, Novak-Frazer L, Rautemaa V, Rajendran R, Sorsa T, Ramage G, et al. A Novel
882 Antifungal Is Active against Candida albicans Biofilms and Inhibits Mutagenic Acetaldehyde
883 Production In Vitro. Bassilana M, editor. PLoS ONE. 2014 May 27;9(5):e97864.

884 51. Muñoz JF, Delorey T, Ford CB, Li BY, Thompson DA, Rao RP, et al. Coordinated host-pathogen
885 transcriptional dynamics revealed using sorted subpopulations and single macrophages infected
886 with Candida albicans. Nat Commun. 2019 Apr 8;10(1):1607.

887 52. Jing H, Liu H, Zhang L, Gao J, Song H, Tan X. Ethanol induces autophagy regulated by mitochondrial
888 ROS in Saccharomyces cerevisiae. J Microbiol Biotechnol. 2018 Dec 28;28(12):1982–91.

889 53. Tsai HJ, Nelliat A. A Double-Edged Sword: Aneuploidy is a Prevalent Strategy in Fungal Adaptation.
890 Genes. 2019 Oct 10;10(10):787.

891 54. Berman J. Ploidy plasticity: a rapid and reversible strategy for adaptation to stress. Munro C, editor.
892 FEMS Yeast Res. 2016 May;16(3):fow020.

893 55. Mba IE, Nweze EI, Eze EA, Anyaegbunam ZKG. Genome plasticity in Candida albicans: A cutting-edge
894 strategy for evolution, adaptation, and survival. Infect Genet Evol. 2022 Apr;99:105256.

895 56. Morard M, Macías LG, Adam AC, Lairón-Peris M, Pérez-Torrado R, Toft C, et al. Aneuploidy and
896 Ethanol Tolerance in Saccharomyces cerevisiae. Front Genet. 2019 Feb 12;10:82.

897 57. Abbey DA, Funt J, Lurie-Weinberger MN, Thompson DA, Regev A, Myers CL, et al. YMAP: a pipeline
898 for visualization of copy number variation and loss of heterozygosity in eukaryotic pathogens.
899 Genome Med. 2014 Nov;6(11):100.

900 58. Kaiser B, Munder T, Saluz HP, Künkel W, Eck R. Identification of a gene encoding the pyruvate
901 decarboxylase gene regulator CaPdc2p fromCandida albicans. Yeast. 1999 May;15(7):585–91.

902 59. Perepnikhatka V, Fischer FJ, Niimi M, Baker RA, Cannon RD, Wang YK, et al. Specific Chromosome
903 Alterations in Fluconazole-Resistant Mutants of *Candida albicans*. J Bacteriol. 1999
904 Jul;181(13):4041–9.

905 60. Selmecki AM, Dulmage K, Cowen LE, Anderson JB, Berman J. Acquisition of Aneuploidy Provides
906 Increased Fitness during the Evolution of Antifungal Drug Resistance. Madhani HD, editor. PLoS
907 Genet. 2009 Oct 30;5(10):e1000705.

908 61. Kukurudz RJ, Chapel M, Wonitowy Q, Adamu Bukari AR, Sidney B, Sierhuis R, et al. Acquisition of
909 cross-azole tolerance and aneuploidy in *Candida albicans* strains evolved to posaconazole. Andrews
910 B, editor. G3 GenesGenomesGenetics. 2022 Aug 25;12(9):jkac156.

911 62. Sun L liu, Li H, Yan T hua, Fang T, Wu H, Cao Y bing, et al. Aneuploidy Mediates Rapid Adaptation to
912 a Subinhibitory Amount of Fluconazole in Candida albicans. Anderson MZ, editor. Microbiol Spectr.
913 2023 Apr 13;11(2):e03016-22.

914 63. Li X, Yang F, Li D, Zhou M, Wang X, Xu Q, et al. Trisomy of chromosome R confers resistance to
915 triazoles in Candida albicans. Med Mycol. 2015 Apr 1;53(3):302–9.

916 64. Yang F, Teoh F, Tan ASM, Cao Y, Pavelka N, Berman J. Aneuploidy Enables Cross-Adaptation to
917 Unrelated Drugs. Malik H, editor. Mol Biol Evol. 2019 Aug 1;36(8):1768–82.

918 65. Cowen LE, Sanglard D, Howard SJ, Rogers PD, Perlin DS. Mechanisms of Antifungal Drug Resistance.
919 Cold Spring Harb Perspect Med. 2015 Jul;5(7):a019752.

920 66. Lee Y, Puumala E, Robbins N, Cowen LE. Antifungal Drug Resistance: Molecular Mechanisms in
921 *Candida albicans* and Beyond. Chem Rev. 2021 Mar 24;121(6):3390–411.

922 67. Holmes AR, Lin YH, Niimi K, Lamping E, Keniya M, Niimi M, et al. ABC Transporter Cdr1p Contributes
923 More than Cdr2p Does to Fluconazole Efflux in Fluconazole-Resistant *Candida albicans* Clinical
924 Isolates. Antimicrob Agents Chemother. 2008 Nov;52(11):3851–62.

925 68. CLSI. Clinical and laboratory standards institute. Reference method for broth dilution antifungal
926 susceptibility testing of yeasts-third edition: Approved standard M27-A3. CLSI Doc M27-A3 Suppl
927 SWayne PA USA. 2008;

928 69. Ford CB, Funt JM, Abbey D, Issi L, Guiducci C, Martinez DA, et al. The evolution of drug resistance in
929 clinical isolates of Candida albicans. eLife. 2015 Feb 3;4:e00662.

930 70. Liu RH, Shang ZC, Li TX, Yang MH, Kong LY. *In Vitro* Antibiofilm Activity of Eucarobustol E against
931 Candida albicans. Antimicrob Agents Chemother. 2017 Aug;61(8):e02707-16.

932 71. Henderson CM, Block DE. Examining the Role of Membrane Lipid Composition in Determining the
933 Ethanol Tolerance of Saccharomyces cerevisiae. Müller V, editor. Appl Environ Microbiol. 2014 May
934 15;80(10):2966–72.

935 72. Vanegas JM, Contreras MF, Faller R, Longo ML. Role of Unsaturated Lipid and Ergosterol in Ethanol
936 Tolerance of Model Yeast Biomembranes. Biophys J. 2012 Feb;102(3):507–16.

937 73. Furutani N, Izawa S. Adaptability of wine yeast to ethanol-induced protein denaturation. FEMS Yeast
938 Res. 2022 Nov 25;22(1):foac059.

939 74. Yang KM, Lee NR, Woo JM, Choi W, Zimmermann M, Blank LM, et al. Ethanol reduces mitochondrial
940 membrane integrity and thereby impacts carbon metabolism of Saccharomyces cerevisiae. FEMS
941 Yeast Res. 2012 Sep;12(6):675–84.

942 75. Tierney KJ, Block DE, Longo ML. Elasticity and Phase Behavior of DPPC Membrane Modulated by
943 Cholesterol, Ergosterol, and Ethanol. Biophys J. 2005 Oct;89(4):2481–93.

944 76. Vu BG, Stamnes MA, Li Y, Rogers PD, Moye-Rowley WS. The Candida glabrata Upc2A transcription
945 factor is a global regulator of antifungal drug resistance pathways. Heitman J, editor. PLOS Genet.
946 2021 Sep 30;17(9):e1009582.

947 77. Yang H, Tong J, Lee CW, Ha S, Eom SH, Im YJ. Structural mechanism of ergosterol regulation by
948 fungal sterol transcription factor Upc2. Nat Commun. 2015 Feb 6;6(1):6129.

949 78. Tan L, Chen L, Yang H, Jin B, Kim G, Im YJ. Structural basis for activation of fungal sterol receptor
950 Upc2 and azole resistance. Nat Chem Biol. 2022 Nov;18(11):1253–62.

951 79. Shrivastava M, Kouyoumdjian GS, Kirbizakis E, Ruiz D, Henry M, Vincent AT, et al. The Adr1
952 transcription factor directs regulation of the ergosterol pathway and azole resistance in *Candida*
953 *albicans*. Goldman GH, editor. mBio. 2023 Oct 4;e01807-23.

954 80. Yang KM, Woo JM, Lee SM, Park JB. Improving ethanol tolerance of Saccharomyces cerevisiae by
955 overexpressing an ATP-binding cassette efflux pump. Chem Eng Sci. 2013 Nov;103:74–8.

956 81. Cherian PP, Schenker S, Henderson GI. Ethanol-Mediated DNA Damage and PARP-1 Apoptotic
957 Responses in Cultured Fetal Cortical Neurons. Alcohol Clin Exp Res [Internet]. 2008 Aug [cited 2023
958 Aug 14]; Available from: https://onlinelibrary.wiley.com/doi/10.1111/j.1530-0277.2008.00769.x

959 82. Chauhan NM, Shinde RB, Karuppayil SM. Effect of alcohols on filamentation, growth, viability and
960 biofilm development in Candida albicans. Braz J Microbiol. 2013 Dec;44(4):1315–20.

961 83. Pfaller MA, Diekema DJ, Messer SA, Boyken L, Hollis RJ. Activities of Fluconazole and Voriconazole
962 against 1,586 Recent Clinical Isolates of *Candida* Species Determined by Broth Microdilution, Disk
963 Diffusion, and Etest Methods: Report from The ARTEMIS Global Antifungal Susceptibility Program,
964 2001. J Clin Microbiol. 2003 Apr;41(4):1440–6.

965 84. Sobel JD. Resistance to Fluconazole of Candida albicans in Vaginal Isolates: a 10-Year Study in a
966 Clinical Referral Center. Antimicrob Agents Chemother. 2023 May 17;67(5):e00181-23.

967 85. Wang WY, Cai HQ, Qu SY, Lin WH, Liang CC, Liu H, et al. Genomic Variation-Mediating Fluconazole
968 Resistance in Yeast. Biomolecules. 2022 Jun 17;12(6):845.

969 86. Morschhäuser J, Barker KS, Liu TT, Blaß-Warmuth J, Homayouni R, Rogers PD. The Transcription
970 Factor Mrr1p Controls Expression of the MDR1 Efflux Pump and Mediates Multidrug Resistance in
971 Candida albicans. Johnson AD, editor. PLoS Pathog. 2007 Nov 2;3(11):e164.

972 87. Nishimoto AT, Zhang Q, Hazlett B, Morschhäuser J, Rogers PD. Contribution of Clinically Derived
973 Mutations in the Gene Encoding the Zinc Cluster Transcription Factor Mrr2 to Fluconazole
974 Antifungal Resistance and *CDR1* Expression in *Candida albicans*. Antimicrob Agents Chemother.
975 2019 May;63(5):e00078-19.

976 88. MacPherson S, Larochelle M, Turcotte B. A Fungal Family of Transcriptional Regulators: the Zinc
977 Cluster Proteins. Microbiol Mol Biol Rev. 2006 Sep;70(3):583–604.

978 89. Junier A, Weeks A, Alcaraz Y, Kumamoto CA. Bypass of Dfi1 Regulation of Candida albicans Invasive
979 Filamentation by Iron Limitation. Mitchell AP, editor. mSphere. 2022 Feb 23;7(1):e00779-21.

980 90. Zhang JD, Ruschhaupt M, Biczok R. ddCt method for qRT–PCR data analysis. Citeseer.
981 2013;48(4):346–56.

982 91. White SJ, Rosenbach A, Lephart P, Nguyen D, Benjamin A, Tzipori S, et al. Self-Regulation of Candida
983 albicans Population Size during GI Colonization. Cormack BP, editor. PLoS Pathog. 2007 Dec
984 7;3(12):e184.

985 92. Illumina. BCL Convert: a proprietary Illumina software for the conversion of BCL files to basecalls.
986 2021;

987 93. Li H. Aligning sequence reads, clone sequences and assembly contigs with BWA-MEM. ArXiv Prepr
988 ArXiv13033997. 2013;

989 94. McKenna A, Hanna M, Banks E, Sivachenko A, Cibulskis K, Kernytsky A, et al. The Genome Analysis
990 Toolkit: A MapReduce framework for analyzing next-generation DNA sequencing data. Genome Res.
991 2010 Sep;20(9):1297–303.

992

993 **Supporting Information**

994 **Supplemental Figure S1: Quantification of small colony variants throughout passaging of**
995 **four separate populations of cells that were exposed repeatedly to increasing**
996 **concentrations of ethanol in medium A or repeatedly exposed to water in medium A.**
997 Quantification of small colony variants throughout passage numbers of four separate
998 populations of cells that were exposed repeatedly to increasing concentrations of ethanol in
999 media A or repeatedly exposed to water in media A. Green squares were repeatedly exposed to
1000 ethanol and black dots were repeatedly exposed to water. Y-axis shows % small colonies
1001 relative to total number of colonies. Bars represent the mean values of the populations at that
1002 passage number. Small colonies were classified as less than 50% of the size of the normal
1003 sized colonies on a plate by eye.

1004 **Supplemental Figure S2: Enc and Wnc survival in 10% ethanol**. Enc and Wnc survival in
1005 10% ethanol. Colonies exposed for 4 hours in 10% ethanol or 10% water and plated on YPD-
1006 agar to count final colonies. The percentage of final colonies in 10% ethanol compared to 10%
1007 water were calculated and used to calculate a relative survival compared to SC5314 within each
1008 experiment (y-axis). Normal-sized colonies from ethanol populations (Enc) or water population
1009 (Wnc) were used. One-way ANOVA with Welch's correction was used for statistical testing with
1010 multiple comparisons. Median values with 95% confidence interval are plotted for 8-16 replicate
1011 cultures from 2-4 separate experiments for each strain.

1012 **Supplemental Figure S3: Growth curves and doubling times of Esc strains and normal-**
1013 **sized colony strains in YPD.** Isolated colonies were picked and grown for 20 hours to post-
1014 exponential phase and seeded into YPD in 96 well plates at an approximate OD600 of 0.05.
1015 Cells were grown for 48 hours at 30ºC with constant shaking in a Biotek Epoch2 plate reader
1016 with OD600 read every 30 minutes. Three biological replicate cultures from each strain were
1017 used to graph the growth curves. Growth curves show the mean and standard deviation of each

1018 timepoint. The wildtype, background strain: SC5314, a culture from the repeat media-A (with no
1019 ethanol exposure) is shown as RepDMEM-2, and a normal sized colony from a repeat ethanol
1020 exposure population is shown as RepEtOH-8. Esc6, Esc7, and Esc8 are all shown as well.
1021 Timepoints 0-24 hours were used to calculate doubling times by performing a nonlinear
1022 regression in GraphPad Prism with the exponential plateau fit to find the rate constant: k. All R^2
1023 values were above 0.9331. k values were then used to calculate doubling times with the formula
1024 LN(2)/k. These were standardized to the SC5314 doubling times and then plotted in this figure
1025 as standardized doubling times.

1026 **Supplemental Figure S4: Principal component analyses for SC5314 vs Esc6, Esc7, or**
1027 **Esc8 in 10% ethanol from RNA sequencing**. Principal component analyses for SC5314 vs
1028 Esc6, Esc7, or Esc8 in 10% ethanol each from RNA sequencing. PC1 variance ranges from
1029 81%-93% and PC2 variance ranges from 4%-9%. SC5314 is shown in red dots in each and Esc
1030 strains are shown in blue. Each dot represents a separate biological replicate culture that was
1031 sequenced.

1032 **Supplemental Figure S5: Gene Ontology Terms of the Top 20 Processes of Significantly**
1033 **Enriched Transcripts in Esc strains exposed to ethanol compared to SC5314 exposed to**
1034 **ethanol**. Gene Ontology Terms of the Top 20 Processes of Significantly Enriched Transcripts in
1035 Esc strains exposed to ethanol compared to SC5314 exposed to ethanol. Transcripts that were
1036 significantly enriched in Esc strains were used to determine GO term process clustering on
1037 Candida Genome Database GO term finder. The top 20 hits from each strain were added to the
1038 graph and shown on y-axis. Esc6 bars are shown in blue, Esc7 bars are shown in black, and
1039 Esc8 bars are shown in orange. X-axis shows the cluster frequency of each of these processes
1040 relative to the total number of genes in the respective sets of enriched transcripts used for the
1041 analysis.

1042 **Supplemental Figure S6: Histogram Fit Curve of Esc6 Allele Depth Ratio.** Histogram fit
1043 curve of Esc6 allele depth ratio is shown. Esc6 is used as an example of what was done for all
1044 of the strains that were sequenced. Binning was performed by calculating the number of genes
1045 that had allele depth ratios within bins of 0.05. The bin of 0-0.05 was set to an arbitrary number
1046 as this represents homozygous for the reference strain and should not be called in the
1047 sequence variant report. Then a trimodal fit was performed in excel and minima values were
1048 calculated and used for further determination of heterozygous and homozygous polymorphisms.

1049 **Supplemental Figure S7: MIC50 values from broth-microdilution experiments of SC5314**
1050 **and Esc6, Esc7, and Esc8**. MIC50 values from broth-microdilution experiments of SC5314 and
1051 Esc6, Esc7, and Esc8. Six separate biological replicate experiments were conducted and
1052 plotted. MIC50 values were determined for each by measuring metabolic activity (XTT) and
1053 determining the well that represented a 50% reduction in metabolic activity. Geometric means
1054 with geometric SD are graphed and ordinary One-way ANOVA was performed for statistical
1055 significance.

1056 **Supplemental Figure S8: Voriconazole Disk-Diffusion Images of SC5314 and Esc Strains.**
1057 SC5314 and Esc strains (-1 and -2 indicate biological replicate cultures) were grown to post
1058 exponential phase and then seeded onto YPD agar at a concentration of 10^5 cells per plate. A 1
1059 ug disk of voriconazole was placed in the center of the plate. These plates were incubated at
1060 30ºC for 48 hours and then imaged with the same settings and converted to black and white
1061 images.

1062 **Supplemental Figure S9: UPC2 to HSP90 Ratio of SC5314 vs Esc7 in different conditions**.
1063 UPC2 to HSP90 Ratio of SC5314 vs Esc7 in different conditions. Arbitrary transcript values from
1064 RNA-seq data were used to calculate transcript ratios of UPC2 to HSP90 and were plotted (y-
1065 axis). Ordinary one-way ANOVA used for statistical significance. NS = not significant. * = p-
1066 value of 0.0377.

1067 **Supplemental Table S1 Transcripts showing significant changes in abundance between**

1068 **SC5314 with ethanol vs water medium by RNASeq**

1069 **Supplemental Table S2 Transcripts showing significant changes in abundance between**

1070 **Esc7 with ethanol vs water medium by RNASeq**

1071 **Supplemental Table S3 Transcripts showing significant changes in abundance between**

1072 **Esc7 with ethanol vs SC5314 with ethanol medium by RNASeq**

1073 **Supplemental Table S4 Transcripts showing significant changes in abundance between**

1074 **Esc7 with water vs SC5314 with water medium by RNASeq**

1075 **Supplemental Table S5 Transcripts showing significant changes in abundance between**

1076 **Esc6 with ethanol vs water medium by RNASeq**

1077 **Supplemental Table S6 Transcripts showing significant changes in abundance between**

1078 **Esc8 with ethanol vs water medium by RNASeq**

1079 **Supplemental Table S7 Transcripts showing significant changes in abundance between**

1080 **Esc6 with ethanol vs SC5314 with ethanol medium by RNASeq**

1081 **Supplemental Table S8 Transcripts showing significant changes in abundance between**

1082 **Esc8 with ethanol vs SC5314 with ethanol medium by RNASeq**

1083 **Supplemental Table S9 Transcripts showing significant changes in abundance between**

1084 **Esc6 with water vs SC5314 with water medium by RNASeq**

1085 **Supplemental Table S10 Transcripts showing significant changes in abundance between**

1086 **Esc8 with water vs SC5314 with water medium by RNASeq**

1087 **Supplemental Table S11 Esc6 Genomic Polymorphisms**

1088 **Supplemental Table S12 Esc7 Genomic Polymorphisms**

1089 **Supplemental Table S13 Esc8 Genomic Polymorphisms**

1090 **Supplemental Table S14: Primers used in this study.**

Figure 1

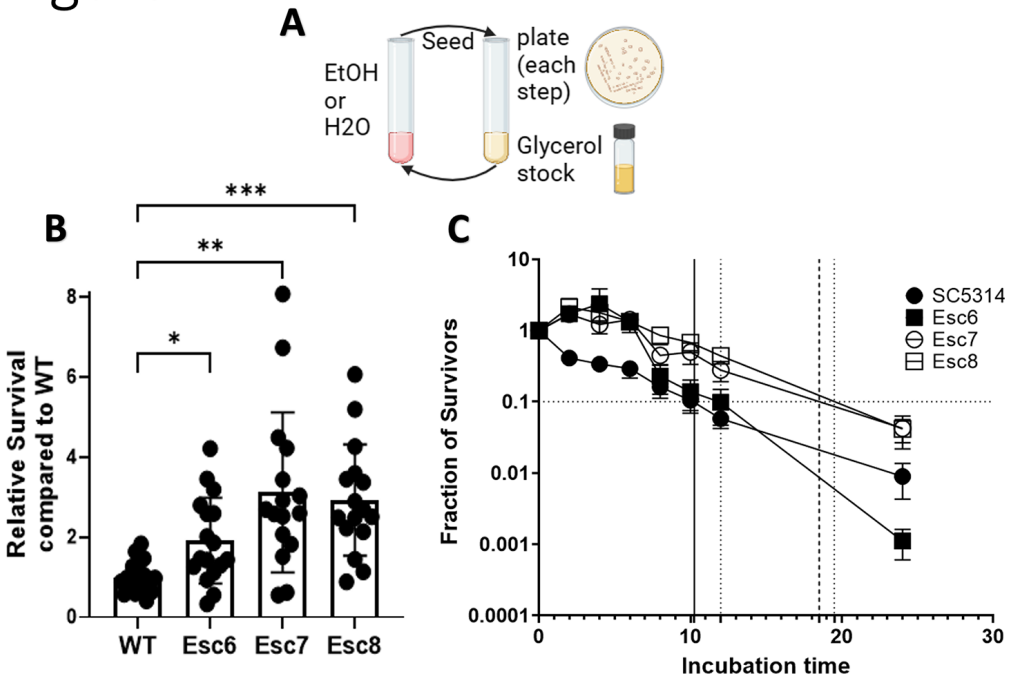
A
Seed
EtOH
or
H2O
plate
(each
step)
Glycerol
stock
B
***
**
*
Relative Survival
compared to WT
0
2
4
6
8
WT
Esc6
Esc7
Esc8
C
Fraction of Survivors
10
1
0.1
0.01
0.001
0.0001
0
10
20
30
Incubation time
SC5314
Esc6
Esc7
Esc8

Figure 2

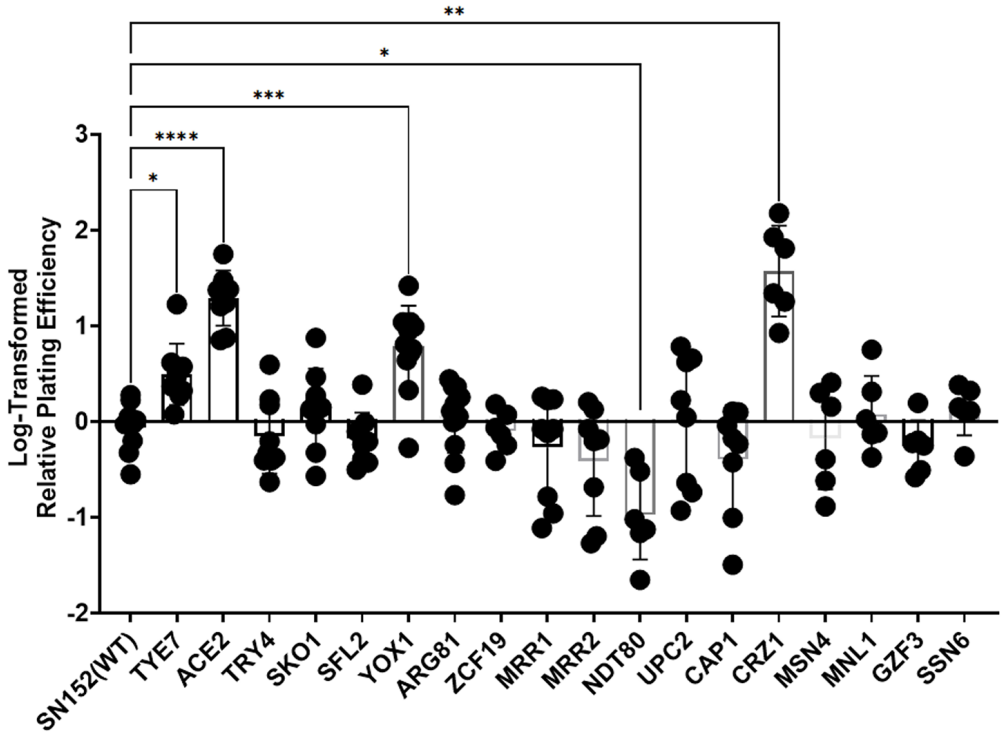
**
*
***
****
*
3
2
1
0
-1
-2
Log-Transformed
Relative Plating Efficiency
SN152(WT)
TYE7
ACE2
TRY4
SKO1
SFL2
YOX1
ARG81
ZCF19
MRR1
MRR2
NDT80
UPC2
CAP1
CRZ1
MSN4
MNL1
GZF3
SSN6

Figure 3

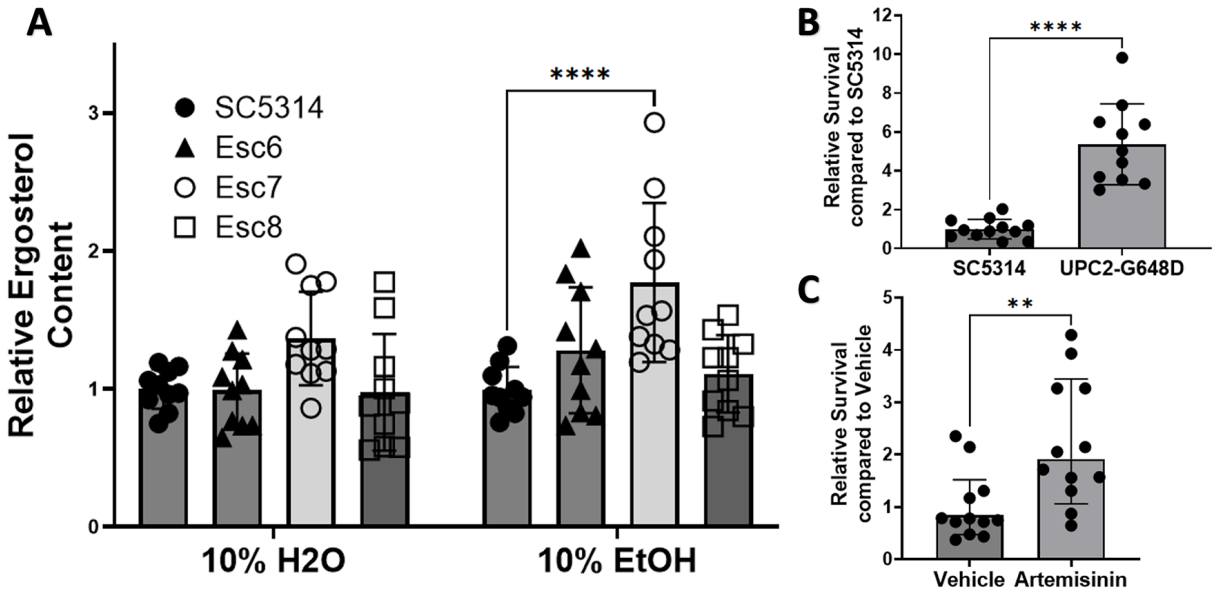
A
Relative Ergosterol Content
SC5314
Esc6
Esc7
Esc8
****
10% H2O
10% EtOH
B
Relative Survival compared to SC5314
****
SC5314
UPC2-G648D
C
Relative Survival compared to Vehicle
**
Vehicle
Artemisinin

Figure 4

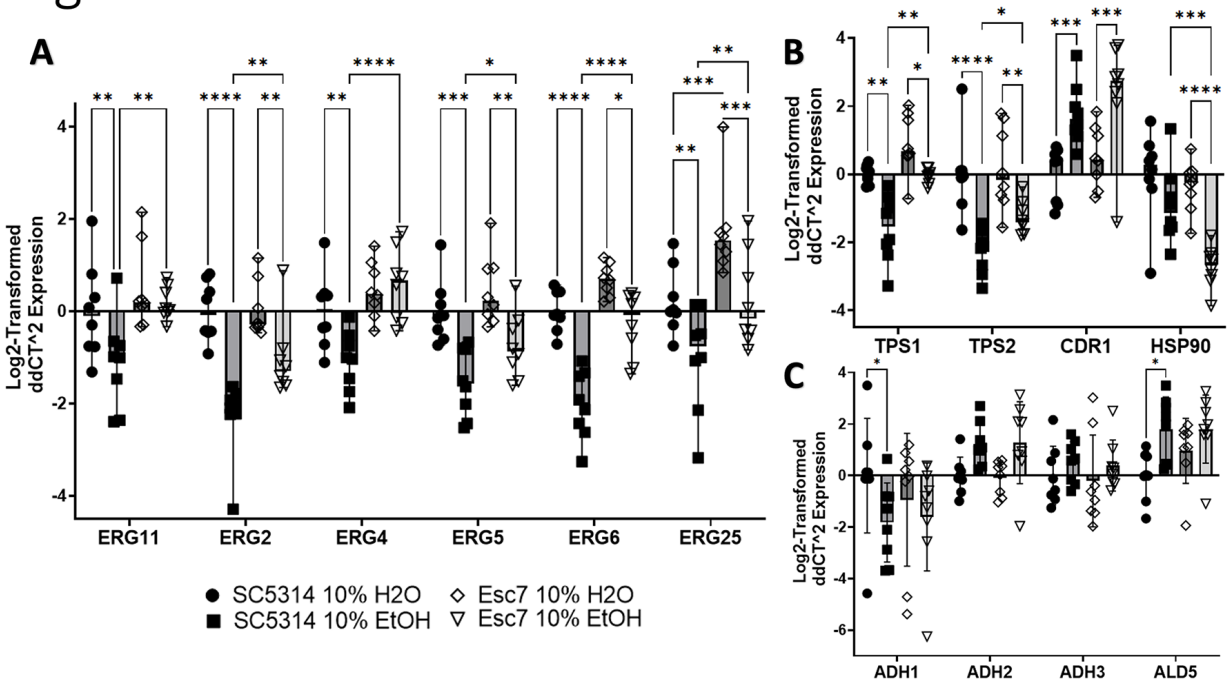
A
B
C
Log2-Transformed ddCT^2 Expression
ERG11
ERG2
ERG4
ERG5
ERG6
ERG25
TPS1
TPS2
CDR1
HSP90
ADH1
ADH2
ADH3
ALD5
SC5314 10% H2O
SC5314 10% EtOH
Esc7 10% H2O
Esc7 10% EtOH

Figure 5

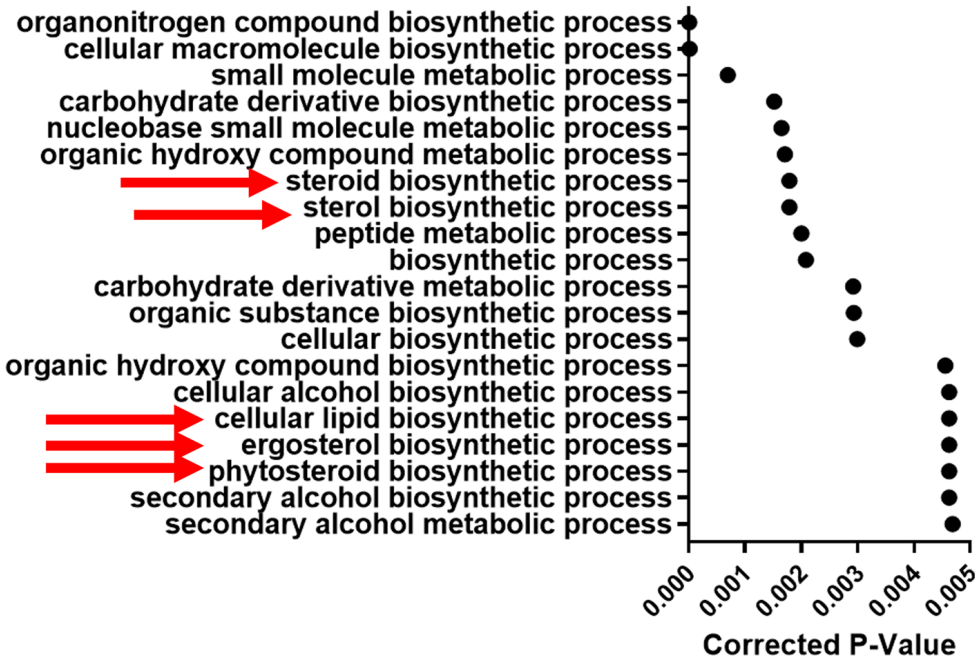
organonitrogen compound biosynthetic process
cellular macromolecule biosynthetic process
small molecule metabolic process
carbohydrate derivative biosynthetic process
nucleobase small molecule metabolic process
organic hydroxy compound metabolic process
steroid biosynthetic process
sterol biosynthetic process
peptide metabolic process
biosynthetic process
carbohydrate derivative metabolic process
organic substance biosynthetic process
cellular biosynthetic process
organic hydroxy compound biosynthetic process
cellular alcohol biosynthetic process
cellular lipid biosynthetic process
ergosterol biosynthetic process
phytosteroid biosynthetic process
secondary alcohol biosynthetic process
secondary alcohol metabolic process
0.000
0.001
0.002
0.003
0.004
0.005
Corrected P-Value

Figure 6

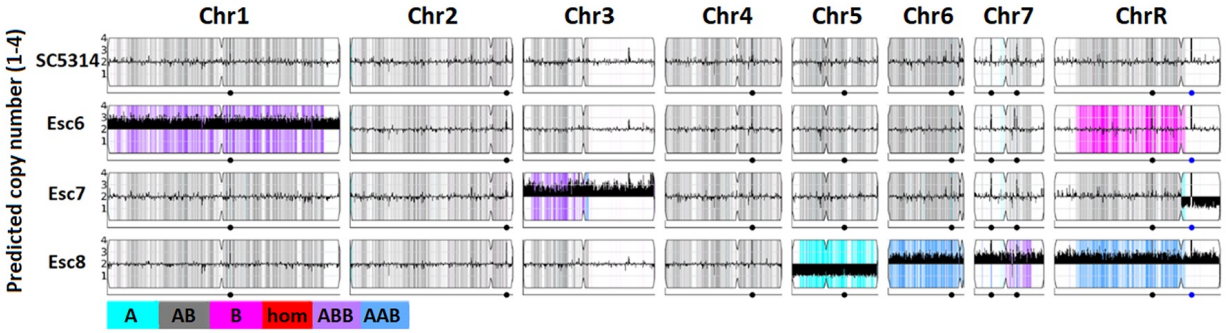
Chr1
Chr2
Chr3
Chr4
Chr5
Chr6
Chr7
ChrR
SC5314
Esc6
Esc7
Esc8
Predicted copy number (1-4)
A
AB
B
hom
ABB
AAB

Figure 7

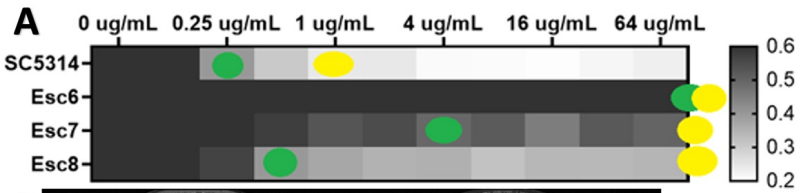

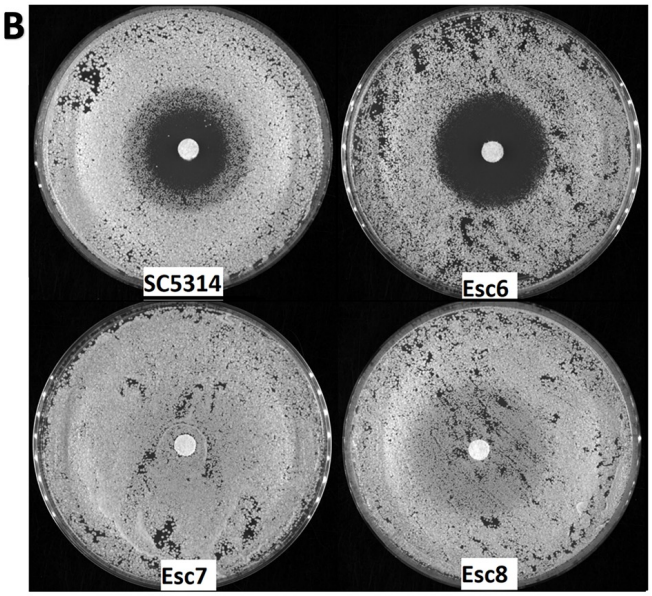

C

Strain	Caspofungin MIC (median)
SC5314	0.032
Esc6	0.016
Esc7	0.032
Esc8	0.064
	Amphotericin B MIC (mean)
SC5314	0.208
Esc6	0.167
Esc7	0.208
Esc8	0.146